WORLD RESOURCES INSTITUTE

TECHNICAL NOTE

Calculating indicators from global geospatial datasets to benchmark and track changes in the urban environment

Eric Mackres, Ted Wong, Saif Shabou, Elizabeth Wesley, and Thet Hein Tun

CONTENTS

Technical notes document the research or analytical methodology underpinning a publication, interactive application, or tool.

Suggested Citation: Mackres, E., T. Wong, S. Shabou, E. Wesley, and T.H. Tun. 2025. "Calculating indicators from global geospatial datasets to benchmark and track changes in the urban environment." Technical Note. Washington, DC: World Resources Institute. Available online at doi.org/10.46830/writn.22.00123v2.

Abstract

Global datasets derived from remote sensing, urban sensors, crowdsourcing, or surveys can provide valuable insights on the current state of cities, how cities are changing, and opportunities to improve the urban environment. This technical note discusses methods for using these data in combination with locally meaningful jurisdictional boundaries to calculate local measurements of indicators on several themes—including access to urban amenities, air quality, biodiversity, flooding, climate change mitigation, heat, and land protection and restoration—relevant to urban decision-makers, researchers, and other stakeholders. The authors identified and prioritized these indicators in consultation with program staff and stakeholders from several global sustainable urban development initiatives: Cities4Forests; UrbanShift; Transformative Urban Coalitions; and Deep Dive Cities from World Resources Institute's Ross Center for Sustainable Cities. We also generated indicator calculations for cities of interest for these initiatives. These indicators can help urban policymakers and civil society assess differences within their cities; make comparisons with other cities; and measure themselves against national or global benchmarks, such as the Sustainable Development Goals, or against self-defined metrics. We applied geospatial analysis and zonal statistics methods to existing published geospatial datasets and relevant administrative, statistical, or physical city boundaries to calculate comparable indicators for any city or urban area. This methodology can be applied to any area of interest on Earth. Most indicators are based on open-source data, increasing the feasibility of repeating, replicating, and scaling the analyses at low marginal cost. Although the transferability and comparability of these methods are notable strengths of this approach, this note also discusses the limitations of this approach for decision-making.

Introduction

Global datasets derived from sources such as remote sensing, urban sensors, crowdsourcing, or surveys can provide valuable insights on the current state of cities, how cities are changing, differences among cities and among neighborhoods within cities, and opportunities to improve the urban environment (Prakash et al. 2020; Helmrich et al. 2021). However, these data are often inaccessible or not immediately relevant to urban stakeholders and decision-makers (Kalluri et al. 2003; Zerger and Smith 2003; Engel-Cox et al. 2004; Wellmann et al. 2020). Processing these data to produce indicators that provide local measurements of themes of interest to local stakeholders is a necessary, yet oftentimes missing, step to enable the supply of new data to meet the demand for locally relevant insights and responsive decision-making (Prakash et al. 2020; Wellmann et al. 2020). Additionally, these indicators can help urban policymakers and civil society assess differences within their cities; make comparisons with other cities; and measure themselves against national or global benchmarks, such as the Sustainable Development Goals (SDGs), or against self-defined metrics (Kuffer et al. 2018; Avtar et al. 2019; Kavvada et al. 2020; Wang et al. 2020; Giuliani et al. 2021; Song and Wu 2021).

The past few years have seen the beginning of a revolution in remote sensing, crowdsourced data, cloud computing, and machine learning—technologies that are quickly generating new insights about Earth and its urban areas (Fritz et al. 2019; Kavvada et al. 2020; Niu and Silva 2020; Salcedo-Sanz et al. 2020; Ludwig et al. 2021). For the first time, researchers and citizen scientists have access to globally standardized, open-source, continually updated datasets and methods to help answer important questions about how we live and the impacts of our present and future activities, from the neighborhood to the continent scale. This also means that some information that had not been previously collected or made public through local methods (e.g., ground-based tree inventories) can be generated through alternative means (e.g., remote sensing–based tree cover mapping), which are often cheaper and easier to implement over large areas. Moreover, using open-source data increases the feasibility of repeating, replicating, and scaling the analyses for additional cities or time frames at low marginal cost, which can be particularly helpful in data-scarce regions or on topics with limited local data available.

To help understand the status of development and sustainability in cities and identify existing and potential challenges, this paper presents a consistent, replicable approach to calculate indicators on seven key themes: access to urban services and amenities (ACC), air quality (AQ), biodiversity (BIO), flooding (FLD), climate change mitigation (GHG), heat (HEA), and land protection and restoration (LND). Data to measure these indicators, as described in this document, were taken almost exclusively from global, open-source datasets. However, these methods can be customized by including equivalent local datasets.

We calculated indicators to assess the baselines and trends of change within each city on identified themes, providing information to distinguish patterns within and between cities and helping to detect problems and define solutions (e.g., prioritizing neighborhoods with limited tree cover for a tree-planting campaign). The methods are open source, so other researchers are also welcome to use the methods and scripts developed to process data and make calculations for other cities or with different input data. The results will be disseminated to local and national governments as well as to civil society stakeholders in the context of initiatives supported by World Resources Institute's (WRI's) Ross Center for Sustainable Cities.

So far, the indicators developed using this framework align with themes of interest of four city cohorts with which WRI Ross Center has been working. The two immediate pilot applications of the indicator methods described in this technical note are for cities participating in the Cities4Forests and UrbanShift initiatives.

- Cities4Forests[1] supports city decision-makers in over 80 cities in making commitments and taking action to preserve and expand tree cover within, near, and far away from their cities. Urban tree indicators can be used by forestry or other tree-focused staff in municipal governments to inform policies and programs related to forests and natural resource management.
- UrbanShift[2] supports city decision-makers across 23 cities on four continents to adopt integrated approaches to urban development, shaping zero-carbon, climate-resilient communities. The initiative's focus includes biodiversity, climate change, and land degradation, and we have developed indicators on these themes. We anticipate that city planning and other strategic sustainable urban investment–focused staff in municipal governments will use the indicators to inform policies, programs, and projects in UrbanShift cities.

The indicators will also support these initiatives of the WRI Ross Center:

- Transformative Urban Coalitions, which facilitates the establishment of coalitions in five Latin American cities to develop new strategies for addressing inequality and other development challenges, while reducing carbon emissions.

- The Deep Dive Cities Initiative, which focuses on locally driven strategic projects as entry points to foster long-term, cross-sectoral, and transformative change. Through the initiative, WRI provides strategic funding and additional technical capacity to support a wide range of projects, from decarbonizing transportation and enhancing climate action to strengthening disaster preparedness and urban resilience.

The themes prioritized and indicators calculated for the city cohorts convened by these initiatives were developed in consultation with their staff and stakeholders. An iterative process involving meetings with and surveys of staff working directly with city stakeholders in 2022 (Cities4Forests account managers and UrbanShift regional coordinators) and 2024 (Deep Dive Cities engagement leads) provided the main information used to identify the most important and relevant themes, define the indicators, and organize the presentation of the calculations for the cities. Indicator calculations and visualizations for these cities are publicly accessible through an online dashboard.

We anticipate that these indicators, and others like them calculated using a similar framework, will be relevant to many other city cohorts and for other urban themes. Many indicators also align with global objectives, such as the urban targets of the Sustainable Development Goals (UN n.d.), the "3-30-300" guidelines for urban greening (Konijnendijk 2021), and the "15-minute city" concept (Moreno et al. 2021). (We briefly describe 3-30-300 and other frameworks in the indicator descriptions below.) We foresee additional uses of the indicators included in this technical note in other geographies and time frames and the development of supplemental indicators on existing and new themes and using new data sources. Additionally, we expect to update the indicator calculation methodologies for these current city cohorts as new data covering additional years become available.

Some cities may have more granular and detailed relevant data for measuring the themes of our indicators. However, even those cities can benefit from measurements that are standardized globally, between cities, and over time; provide enhanced temporal resolution; and are available worldwide. Additionally, these indicators can provide a screening and prioritization tool. Global data will rarely, if ever, be more useful than local data for monitoring local dynamics, but such datasets can help users understand the main challenges faced locally and start conversations about addressing them. Even when the lower local accuracy levels of global datasets impede local usability, they can help generate the conversations needed to identify local concerns and then identify better data.

Other projects on various urban and nonurban topics have developed indicators using zonal statistics derived from global geospatial datasets (Bocher et al. 2018; Jing et al. 2019; Cochran et al. 2020; Kuffer et al. 2020; Sathyakumar et al. 2020; Boeing et al. 2022; Nicoletti et al. 2022). However, this publication presents the first method of this kind developed by WRI to include multiple urban themes and focus on the needs of specific city cohorts and their questions around urban change, opportunities, and risks.

Methods

Selection of relevant input datasets

For several indicators, multiple potential source datasets could be used. To select the datasets for use in our indicators, we followed a few general principles. We typically chose the dataset that met the greatest number of our criteria. In cases where there were trade-offs among multiple criteria, we prioritized the criteria that were most important to enable consistent and meaningful calculations of the specific indicator. We used the following criteria to evaluate datasets:

- Published in a peer-reviewed source
- Open-source license
- Globally consistent coverage
- Recency of data
- High spatial resolution
- High accuracy compared with peer data
- Broad temporal coverage (multiple years of data to enable time series comparisons)
- Likelihood of ongoing support for the source data initiative and future updates to the dataset, enabling updates to the indicators and tracking over time
- Compatible spatial and temporal resolution with other datasets used for the indicator

To calculate the indicators, we used a general data management workflow that we consistently applied across all indicators. We also used methods to process specific data relevant to individual indicators. We assigned all indicators short name designations and organized them into themes, as shown in Figure 1. The definitions and methodologies we used to calculate the indicators in the seven themes below are described in detail in the following sections, which are organized and named by theme.

- Access to urban services and amenities

- Air quality
- Biodiversity
- Flooding
- Climate change mitigation
- Heat
- Land protection and restoration

These themes and indicators are not intended to be exhaustive; rather, they are tailored to the needs of the specific initiatives for which they were originally developed. We anticipate adding indicators under these themes and potentially adding themes as they are identified as important by cities or other stakeholders. All indicators are subject to limitations and uncertainty associated with their methods, as described specifically in each indicator section and generally in the "General limitations" section.

General data management workflow

Our general data workflow consisted of five steps to process data, as illustrated in Figure 2.

- **1: Input source data and boundaries.** We calculated the indicators from a variety of sources of global data, and for particular zones, or areas of interest. We defined zones based on locally relevant administrative boundaries. For each city, we defined boundaries for two administrative levels: the overall area of interest (typically a municipality or a metropolitan area) and several subareas (typically multiple wards or districts within a municipality or multiple municipalities within a metropolitan area). The former represents the union into a single polygon of the multiple geographies of the latter. In most cases, we obtained the sources of these boundaries from a polygon file or map received from the local government or from a national statistical agency. If such a local data source was not easily accessed, we retrieved the boundaries from a global database such as geoBoundaries (Runfola et al. 2020) or

Figure 1 | **Themes and indicators described in this document**

THEMES	Access to urban services & amenities	Air quality	Biodiversity	Flooding	Climate change mitigation	Heat	Land protection and restoration
INDICATORS	Recreational space per capita	Air pollutant emissions and costs	Natural areas	Exposure to coastal and river flooding	Greenhouse gas emissions	Future heatwave frequency	Permeable areas
	Residential prevalence of tree cover	High pollution days	Habitat connectivity (landscape coherence)	Future extreme-precipitation days	Greenhouse gas impact of trees	Future extreme temperature	Tree cover
	Urban open space for public use	Fine particulate matter exposure (area-weighted)	Habitat connectivity (effective mesh size)	Land near natural drainage		Land surface temperature	**Vegetation-covered land**
	Hospitals per 1000 residents	Fine particulate matter exposure (population-weighted)	Biodiversity in built-up areas (birds)	Impervious surfaces		Surface reflectivity	Water-covered land
	Proximity to public open space		Change in number of vascular plant species	Vegetation cover in built areas		Built land without tree cover	Habitat areas restored
	Proximity to public green open space		Change in number of bird species	Vegetation cover in riparian zones		Vegetated area	Habitat types restored
	Area of tree-covered land per resident		Change in number of arthropod species	Vulnerability of steep slopes			Protected areas
	Proximity to schools						Protection of Key Biodiversity Areas
	Proximity to goods and services						Built-up Key Biodiversity Areas
	Proximity to potential employment						
	Potential employers within convenient proximity						
	Proximity to public transportation						
	Proximity to healthcare						

Source: WRI authors.

OpenStreetMap (OSM).[3] Where multiple options were available, we consulted stakeholders, generally through WRI country offices and the managers of program partners, on the most appropriate boundaries to use. We also considered maps of the extent of regional urban agglomerations as an alternative definition of the city boundary, using urban-extent areas as classified from built-up density by Angel et al. (2024). For indicators that use a time series of data and for regions where boundaries may have changed over time, we used only the most recent available boundaries for our calculations to hold the region of study constant. We then saved the boundaries for each area of interest as GeoJSON files with a standard naming schema.

The sources of the global data required to calculate each indicator are described with the indicators, below. We obtained some data through application programming interfaces (APIs) maintained by the organizations providing the data. API-derived data include species-observation data from the Global Biodiversity Information Facility, locations of urban amenities and street networks from OpenStreetMap, and air-pollutant concentrations from the Copernicus Atmosphere Monitoring Service. We retrieved some data from Google Earth Engine (GEE) (Gorelick et al. 2017), which collects, stores, and provides researchers with a rich collection of environmental data. GEE-served data include population estimates from WorldPop, the NEX-GDDP-CMIP6[4] downscaled climate simulation outputs, and reflectance and greenness data from the Sentinel-2 satellite mission (ESA 2015b). We obtained some data directly from data-providing organizations. We stored these data for our use in calculating indicators. These data include the Key Biodiversity Areas from BirdLife International and concentrations of fine particulate matter from the Atmospheric Composition Analysis Group at Washington University in St. Louis. The specific datasets named here are only a subset of the datasets in each category, and we provide more detailed descriptions and citations in the indicator descriptions. We also obtained metadata to accompany the data, and we make information from the metadata available with the indicators.

- **2–3: Compute and store layers and indicators.** From the source data, we calculated layers and indicators. Layers are spatially explicit data, calculated for the entire area of interest, which can be useful for understanding the spatial pattern of environmental or social factors relevant to city decision-making. Layers take the form of raster data (stored in GeoTIFF format) or vector data (stored as GeoJSON files). Indicators are data that summarize or synthesize layer data, calculated as a single numerical value either for the entire area of interest or each administrative district. Indicators are stored as tables. We used the defined boundary extents to extract the data for each city area of interest from global datasets relevant to calculating one or more indicator.

  We processed the source data into layers and calculated the indicators from layers using Python scripts that call on a collection of open-source libraries written in Python, R, and Java. All Python scripts and their dependencies are made available through the Cities Indicators Framework (CIF).[5] We stored layer datasets and indicator tables for each city, using a common data schema to facilitate provision of data through the CIF API. Storage is currently in a set of S3 (Simple Storage Service) buckets provided by Amazon Web Services.

- **4–5: Publish and visualize.** Layer and indicator data for any of our project cities, along with metadata, are available through the Cities Indicators API.[6] Data can also be visualized in the CitiesMetrics Dashboard,[7] which provides a user-friendly interactive interface for viewing data as maps and tables; comparing data among cities; and downloading layer data, indicator data, and map images.

Disaggregation and time series

We calculated and report some indicators for a variety of subpopulations or years of interest.

For indicators that describe the exposure of city residents or built-up areas to environmental hazards or proximity of city amenities to residents, we calculated indicator values for both the general population and separately for some subpopulations that might vary in their vulnerability to hazards or their need to make use of amenities. The subpopulations for which we made these calculations are children, elderly persons, female persons, and residents of areas with informal development.

Some indicators are based not on population, but on area of land. For several heat-related indicators (HEA-3–HEA-5, which address land surface temperature, surface reflectivity, and vegetation), we report indicators calculated for total city area and for the subset of the city area that is simultaneously classified as built-up and having informal development. These indicators address heat hazards that are of particular concern in built-up areas, and informality in built-up areas is a vulnerability class for which we wish to provide separate information.

For indicators for which we have more than one year of data, we allow users to choose years of interest. We report some indicators as time series and provide values as tables and multiyear plots. Indicators that are reported as time series include those

Figure 2 | **General data management workflow**

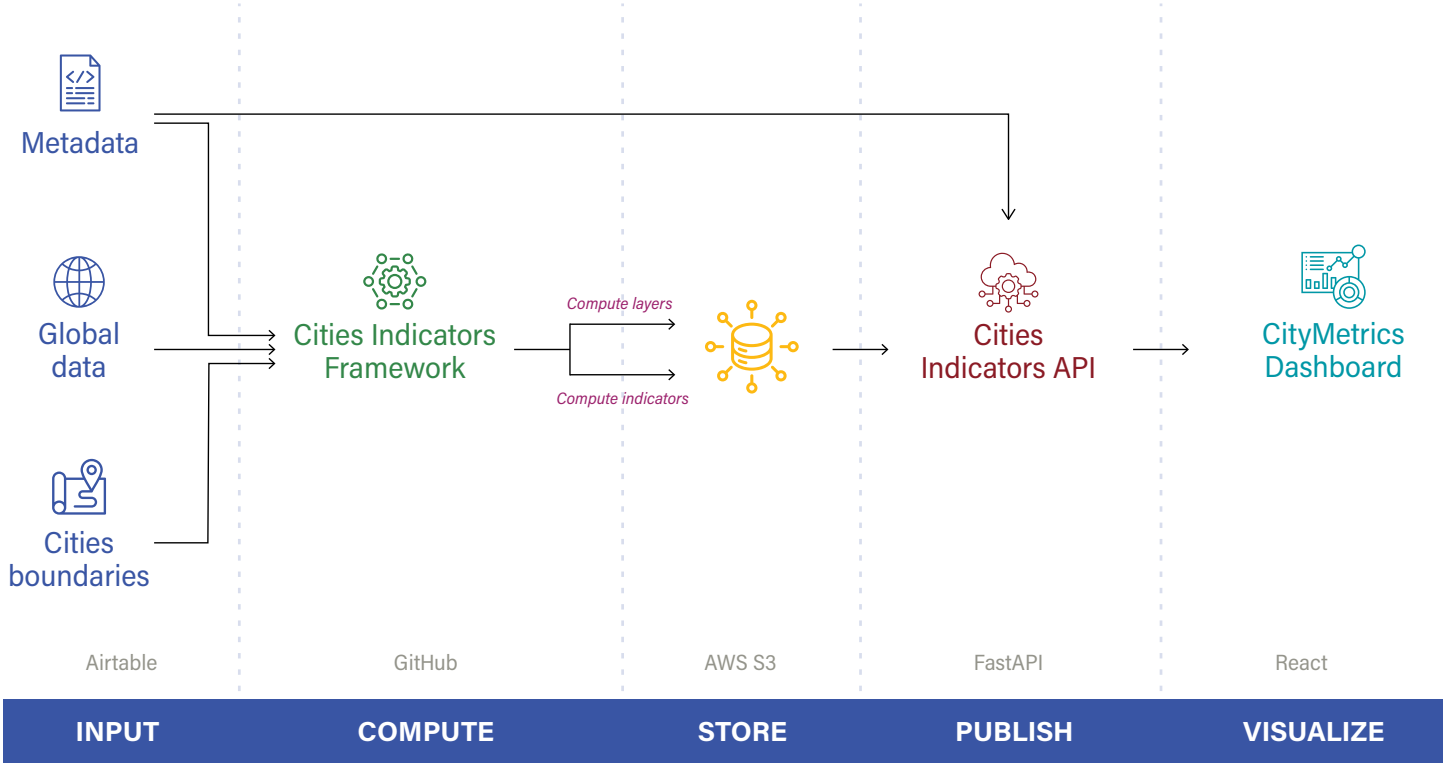

Notes: Abbreviations: AWS = Amazon Web Services; S3 = Simple Storage Service; API = application programming interface. The figure describes the steps we applied to generate calculations for each city, data source, and indicator. We used boundaries to extract a spatial subset layer from the source dataset that is relevant to the city. We then stored this subset and added its metadata to a data catalog. We applied the indicator methods to the spatial subset, and appended the calculation result for each boundary to a table that stores the unique indicator results for each boundary.

Source: WRI authors.

describing concentrations of greenhouse gases and other pollutants, estimates of species richness, and indicators built on estimates of vegetative cover.

Indicators

Access to urban services and amenities (ACC)

Cities exist because the physical proximity of many kinds of activities enables residents to more easily access opportunities and collaborate economically. But access to opportunities varies considerably within cities. These indicators measure the variation in physical access to services and amenities within cities. Amenities in this paper include parks, schools, health care facilities, public transportation stops, places for the purchase and sale of goods and services, and places that are likely to provide jobs to city residents.

While indicators ACC-1 through ACC-5 assess the availability of amenities without regard to travel time within the city, indicators ACC-6 through ACC-13 assess the proximity of urban amenities to city residents' homes. The general method for our proximity indicators was to do the following:

1. Find the locations of the amenities
2. Find information on the city's transportation networks
3. Estimate zones describing locations from which a person can access at least one amenity location within a given period—in which case we call the zones *isochrone areas*—or within a given travel distance via a given transportation mode—in which case we call the zones *isodistance areas*
4. Estimate the fraction of the population residing within the isochrone or isodistance areas

Travel times, distances, and travel modes used for isochrone and isodistance estimates can be customized for particular applications. To date, we have implemented these indicators only for

walking and bicycling. Our implementation can distinguish between pedestrian-accessible and pedestrian-inaccessible roadways, as coded by citizen mappers in OpenStreetMap. Future iterations of this work will calculate isochrone areas and isodistance areas for vehicles in nearly the same way as for walking, but with different travel speeds and consideration of one-way streets. Future iterations of this work will also incorporate routing and service-frequency data from public transit agencies, and will allow us to address the accessibility of urban amenities via bus, metro, and train. Higher values are associated with greater or more inclusive access to essential urban amenities.

For most of the amenity classes we address, we calculated accessibility for at least the 15-minute walking and bicycling isochrone areas and the 400 meter (m) walking isodistance area. The 15-minute isochrone areas support cities in assessing alignment with the concept of the 15-minute city, which is that all city residents should live within a 15-minute walk or bicycle ride of all essential urban amenities (Moreno et al. 2021). The 400 m isodistance areas support assessment under Indicator 1.2.1 of the Global Urban Monitoring Framework, which addresses "the proportion of population living in households with access to basic service" (UN-Habitat 2022). Some accessibility indicators include additional distances and/or travel times to support assessment against other well-known frameworks such as the Sustainable Development Goals and the 3-30-300 guidance for urban greening. These alignments are described with the relevant indicators.

These accessibility indicators are not meant to assess the overall use of the amenities of interest. Rather, we intend to assess the ease with which a city resident could access an amenity by walking, bicycling, or (in future versions of this work) taking public transportation. City residents who have private vehicles might have easy access to larger areas of cities and greater varieties of schools, businesses, and other amenities. However, as poorer people often lack access to private vehicles, an assessment of equitable access to urban amenities focuses on access by foot, bicycle, and public transportation.

ACC-1: recreational space per capita

DEFINITION

The hectares of recreational space (open space for public use) per 1,000 people.

IMPORTANCE

Parks, natural areas, and other open spaces provide city residents with important recreational, spiritual, cultural, and educational services. The use of open and green spaces has been shown to improve human physical and psychological health (Pietilä et al. 2015; Litwiller et al. 2016).

METHODS

We calculated the recreational services indicator using the following equation:

$$\frac{\text{total area of recreational space within the boundary}}{\text{population within the boundary} \div 1{,}000}$$

We took data on recreational areas from the crowdsourced data initiative OSM using the OSMnx library (Boeing 2024). The OSM tags used to retrieve polygons of these areas were *park*, *nature_reserve*, *common*, *playground, pitch,* and *track* in the leisure category and *protected_area* and *national_park* in the boundary category. Population data are 2020 unconstrained estimates from WorldPop accessed through Google Earth Engine (WorldPop n.d.).

LIMITATIONS

WorldPop's global gridded unconstrained dataset is built from the disaggregation of governments' census data. The unconstrained data, which consider all land area rather than only areas with satellite-detectable settlements, can underestimate populations in some urban areas. For example, analysis of these WorldPop data for Namibia has found large cell-level errors, particularly in areas of informal settlements (Thomson et al. 2022). We used the unconstrained dataset rather than the settlement-constrained dataset because it is more likely to be updated regularly. If a regularly updated, constrained population dataset becomes available, we may choose to use it.

OSM is a crowdsourced dataset with a diverse user community, and its completeness, accuracy, and standards of use vary considerably. Accuracy within individual studied cities is not precisely known. Some regions lack data on some of their open spaces in OSM, but all cities we have analyzed so far have data on the sites of at least some open spaces. Additionally, local contributing communities use the OSM taxonomic system of tags to categorize features differently. In selecting the tags used in our methods, we considered the most commonly used tags to designate open spaces available for public use (e.g., parks, athletic fields) but attempted to exclude tags used primarily for private, limited access or indeterminate open spaces. However, as the OSM tagging system is not designed to make this distinction, this may result in the exclusion of data on some open spaces

that are available for public use as well as the inclusion of some nonpublic open spaces for some cities. OSM is being constantly edited, potentially improving the relevant data for these cities, so our download of data from one point in time may become outdated. Finally, metadata for OSM features (e.g., parks, roads) include when the feature was added or edited in the map but typically do not provide information on when it was installed on the ground. This makes it difficult to measure changes to cities over time using OSM data.

We considered only recreational open space (generally parks) for this indicator, so smaller recreational facilities like gymnasiums, recreation centers, and smaller swimming pools were excluded. City residents typically have access to more recreational opportunities than are found in recreational open space.

ACC-2: area of tree-covered land per resident

DEFINITION

The area of land with tree canopy of at least 3 m in height per city resident.

IMPORTANCE

Trees provide city residents with numerous benefits, like cooling through shade and evaporative cooling, mitigation of air pollution and noise pollution, and support for local biodiversity with its attendant benefits. Without attempting to quantify these benefits, this indicator reflects the benefit conferred on residents by the areal prevalence of tree canopy in the city or district.

METHODS

For population data, we used the unconstrained gridded population for 2020 at a 100 m resolution from the WorldPop project as retrieved from Google Earth Engine. For tree cover, we used tree cover data from the Meta-WRI Global Canopy Height dataset (Tolan et al. 2024). We reduced the spatial resolution of the 1 m tree-height dataset to align with the 100 m population dataset. In so doing, we considered a 100 m pixel to represent 30 percent canopy coverage when at least 30 percent of the 1 m pixels represented 3 m or more of canopy height. The 30 percent threshold aligns with the Nature Based Solutions Institute's 3-30-300 rule (Konijnendijk 2021), which is that every city resident should live within line of sight of at least three trees, that neighborhoods should have at least 30 percent tree cover, and that every resident should live within 300 m of green open space.

There is no standard tree height for defining urban canopy. We used a 3 m minimum because in urban settings a tree that is at least 3 m in height can cast a downward shadow on pedestrians. We divided the area of the city with tree canopy at least 3 m in height by the number of residents.

LIMITATIONS

Tolan et al.'s (2024) method for estimating tree canopy height was developed and tested for the assessment of forests and agroforests for carbon management, not specifically for monitoring sparsely vegetated areas like cities. The Meta-WRI Global Canopy Height dataset is based on analysis of recent historical satellite data, and its usefulness for long-term change detection depends on future updates. As with all data derived from automated analysis of satellite data, these data are subject to error. The estimated mean absolute error in tree canopy height in this dataset is 2.8 m.

ACC-3: residential prevalence of tree cover

DEFINITION

The percentage of the populated areas with tree cover of at least 3 m in height for greater than 30 percent of the area.

IMPORTANCE

Residential prevalence of tree cover is an important indicator of quality green space, whether the trees are in public or private space. Privately maintained trees also provide a variety of public benefits, including improved air quality, heat mitigation, and shade. In addition to providing a range of ecosystem services, urban forests are increasingly recognized for their socioeconomic benefits (Kondo et al. 2017; Martinuzzi et al. 2018, 2021; Volin et al. 2020). To align with the 3-30-300 concept (Konijnendijk 2021), this indicator considers the 30 percent canopy coverage rule. Note that we calculated this indicator based on area, not population.

METHODS

For population data, we used the unconstrained gridded population for 2020 at a 100 m resolution from the WorldPop project as retrieved from Google Earth Engine. For canopy coverage, we used tree cover data from the Meta-WRI Global Canopy Height dataset, which estimates tree canopy height from satellite data from the years 2009–20 and estimates tree heights within each 1 m pixel (Tolan et al. 2024). For every pixel in the population dataset, we examined the canopy-height pixels within a distance of 300 m (in a study of the 3-30-300 rule, Owen et al. [2024] used a 300 m distance to define neighborhoods). If at least 30 percent of the canopy-height pixels within this distance indicated a tree canopy height of at least 3 m, we

counted the focal population pixel as meeting the "30" rule. The indicator value is the sum of the values of the population pixels that met the rule, divided by the sum of all the population pixels within the city boundary.

We report this indicator using the total population, as well as the population disaggregated by sex and age class, and by informality of residential settlement. For assessing proximity for particular sexes or age groups, we used WorldPop's age- and sex-disaggregated unconstrained 100 m population estimates. We defined children as persons aged 0–14, which is the age grouping for children used by the United Nations (UN) Department of Economic and Social Affairs (UN DESA 2022). We defined elderly persons as those aged 60 or more years, again in alignment with UN practice (UN DESA 2022). To assess proximity for residents of informal settlements, we used the WorldPop estimates for regions identified as *informal development* in the Intraurban Land Use dataset (Guzder-Williams et al. 2023).

LIMITATIONS

For this indicator, we used a global neighborhood definition that does not conform to how many people perceive or experience their neighborhoods. An indicator using local data might be based on formal or resident-provided neighborhood boundaries.

Informality in the Intraurban Land Use dataset is based on the morphological characteristics of buildings as seen in satellite imagery. It therefore does not directly assess the provision of formal services to residents.

ACC-4: urban open space for public use

DEFINITION

The percentage of the urban extent that is open space for public use.

IMPORTANCE

The availability and area of public open space, such as parks, are key factors for assessing the quality of life for city residents. Open spaces provide ecosystem services, recreation opportunities, and habitat for wildlife. Indicators of open space are included in the SDGs (Indicator 11.7.1) (UN-Habitat 2020), the Singapore Index on Cities' Biodiversity (Chan et al. 2021), and the IUCN Urban Nature Indexes (IUCN 2023).

This indicator differs from ACC-1 in that it considers the percentage of land area devoted to public use, rather than the area per resident (or per 1,000 residents).

METHODS

For this indicator, we used polygon data on categories of open space as retrieved from OSM using the OSMnx library (Boeing 2024). The OSM tags used to retrieve these areas were *park, nature_reserve, common, playground, pitch,* and *track* in the leisure category and *protected_area* and *national_park* in the boundary category. For this indicator, we focused on open space that is within urbanized areas of the city and therefore more easily accessible by a greater population. This is distinct from ACC-1, which considers all public open space within the jurisdictional boundary, including in nonurbanized areas. To constrain our analysis to urbanized areas of the city (areas where land is predominantly covered by urban infrastructure, such as buildings and streets, and where most people live and work), we used data on these areas as derived from the urban extents dataset from Angel et al. (2024) to estimate total metropolitan area. This dataset estimates boundaries of the metropolitan area based on automated classification of satellite imagery. One advantage of using this dataset instead of built-up areas within the jurisdictional boundary is that it includes land that would be excluded by the built-up classification in the ESA WorldCover 10 m 2021 V200 land-classification map (ESA 2020a, 2020b; Zanaga et al. 2021).

LIMITATIONS

Because of the relatively high (10 m) resolution of the WorldCover dataset and its definition of built-up areas, large- and medium-sized urban open spaces that are predominantly green areas were excluded. As a result, this indicator best captures smaller open spaces, such as pocket parks; open spaces that are not predominantly green, such as plazas; and designated parks that are a mix of built-up and nonbuilt land, such as historic districts. This indicator is a candidate for future revision to use an alternative urbanized area mask based on a dataset that provides a common, global definition of urbanized areas of cities that is less restrictive of green open spaces. See the above discussion of the urban extents dataset.

The limitations of OSM described in ACC-1 apply here as well.

ACC-5: hospitals per 1,000 residents

DEFINITION

The number of hospitals per 1,000 residents.

IMPORTANCE

The availability of hospital beds is essential for planning for disasters and other major health crises. This indicator supports long-term planning for the availability of health care.

METHODS

For hospital locations, we queried OSM for *hospital* in the amenity category. Points that were within 0.001 degrees of each other (approximately 100 m) were considered duplicates; all but one duplicate were removed. We estimated the city's population as the sum within city boundaries of the pixel values from WorldPop's unconstrained population estimates, and calculated the indicator using the following equation:

$$\frac{\text{number of hospital points}}{\text{population} \div 1{,}000}$$

LIMITATIONS

The limitations previously described for OSM data and WorldPop's unconstrained population estimates apply to this indicator.

This analysis does not consider the capacity, quality, or geographical accessibility of hospitals.

ACC-6: proximity to public open space

DEFINITION

The percentage of the population within a 300 m walk, 400 m walk, 15-minute walk (1,125 m), or 15-minute (3 kilometer [km]) bicycle ride of public open space.

IMPORTANCE

Beyond simply being present, open space must also be easy to access. Although accessibility has many elements, physical proximity to open spaces is an important factor affecting who does or does not have access. The spatial distribution of open spaces across a city, their alignment with population locations, and their accessibility within walking distance are all critical factors for understanding how many city residents are well served by open space. In addition to addressing the 15-minute walking and bicycling isochrone areas, we calculated this indicator using a 300 m isodistance area in alignment with the 3-30-300 rule (see ACC-2) and a 400 m isodistance area in alignment with SDG 11.7.1 (UN n.d.). Fifteen minutes by foot or bicycle corresponds in our estimates to 1,125 m and 3 km, respectively. This indicator can also be calculated using distance or travel time via modes of transportation other than walking and bicycling.

We report this indicator using the total population, as well as the population disaggregated by sex and age class, and by informality of residential settlement. To assess proximity by sex and age group, we used WorldPop's age- and sex-disaggregated unconstrained 100 m population estimates. To assess proximity for residents of informal settlements, we used the WorldPop estimates for regions identified as *informal development* in the Intraurban Land Use dataset.

METHODS

This indicator makes use of global unconstrained gridded population at a 100 m resolution from the WorldPop project as accessed on Google Earth Engine (WorldPop n.d.). We retrieved the sampled points on the perimeters of the open space polygons from OSM as in ACC-1. We then used these points as focal points to generate isochrone-area and isodistance-area polygons by the R package r5r (Pereira et al. 2021) or the Python package r5py (Fink et al. 2022). We estimated travel times for a given network of streets and roads, which we obtained from OSM. The population within an isochrone or isodistance area was calculated and then converted to a percentage by dividing that value by the total population of the area of interest. The r5r and r5py packages can calculate isochrones for different travel times and different travel modes. For public-transit travel times, transit-network information for the city in question must be provided to r5r and r5py in the form of a General Transit Feed Specification (GTFS) file.

We determined walking time using a walking speed of 4.5 km/hour, the median walking speed in data collected by Schimpl et al. (2011). For bicycle speed, we used 12 km/hour, which is the default bicycle speed in r5r (Saraiva et al. 2025).

LIMITATIONS

The previously described limitations of OSM data, WorldPop's unconstrained population estimates, and assessments of informality in the Intraurban Land Use dataset are also relevant to this indicator. WorldPop's age- and sex-disaggregated population estimates are based in part on census data and in part on a statistical model based on a variety of spatial covariates (Alegana et al. 2015). This modeling was developed with rural applications in mind and might include unknown biases.

The r5r and r5py packages' travel-time estimates are based only on roadway geometry and type (and, in the case of public transit, any available GTFS data on service frequency). They do not consider roadway conditions, climate, topography, or other environmental factors that affect the ability of persons or vehicles to move through transportation networks. These estimates should therefore be considered best-case estimates.

ACC-7: proximity to green public open space

DEFINITION

The percentage of the population within a 300 m walk, 400 m walk, 15-minute walk (1,125 m), or 15-minute (3 km) bicycle ride of vegetated public open space.

IMPORTANCE

Trees and other vegetation confer benefits on urban residents, including cooling, mitigation of air pollution and noise pollution, beauty, and habitat for local biodiversity. This indicator is identical to ACC-6, but considers only the subset of open space that is largely vegetated.

METHODS

Calculation of this indicator is identical to that for ACC-6, except that it considers only the open spaces that meet at least one of these two criteria:

- At least 30 percent of the area within the open space includes tree cover 3 m or greater in height
- At least 30 percent of the area within the open space has fractional vegetation of at least 0.5.

Fractional vegetation (*F*r) is a measure of the areal fraction of a patch of land that is covered by living plants calculated using data from the Normalized Difference Vegetation Index (NDVI). It is a well-respected measure that outperforms many other vegetation indicators in being robust both to soil noise and to scale effects (Gao et al. 2020). Using the method of Carlson and Ripley (1997), we calculated *F*r for each pixel using the following equation:

$$F_r = \left(\frac{NDVI_{90} - NDVI_{nonveg}}{NDVI_{veg} - NDVI_{nonveg}} \right)^2$$

where the so-called *endmembers*, $NDVI_{veg}$ and $NDVI_{nonveg}$, are the NDVI in pixels representing fully vegetated and completely unvegetated patches, respectively. Most researchers establish endmembers by manually selecting vegetated and unvegetated locations within their areas of interest (e.g., Song et al. 2022; Wesley and Brunsell 2019; Amiri et al. 2009). Zeng et al. (2000) suggest an approach to finding locally appropriate endmember values from remote-sensing data, using percentile values of NDVI measurements. To avoid NDVI variability associated with artifacts and from seasonal changes in vegetation, we created and used a composite image of the 90th-percentile NDVI value, $NDVI_{90}$, of the area of interest. We calculated the percentiles for each pixel over all the days in the calendar year, using only cloud-free pixels. Using percentile values from Gao et al. (2020), we took as endmembers the 75th-percentile $NDVI_{90}$ value of all pixels classified in the Dynamic World vegetation-classification dataset (Brown et al. 2022) as either tree, grass, or scrub and shrub for $NDVI_{veg}$, and for $NDVI_{nonveg}$, the 5th-percentile $NDVI_{90}$ for pixels classified as built-up in Dynamic World. We also used $NDVI_{90}$ in the calculation of *F*r.

As with ACC-3, we calculated this indicator using population disaggregated by sex and age class, and by informality of residential settlement.

LIMITATIONS

The limitations of ACC-3 apply to this indicator.

Our method of defining *open green space* is based on global data and can fail to account for important factors affecting accessibility by the public and provision of the benefits of urban nature. For example, it does not distinguish between woodlands and patches dominated by turf and therefore would treat sport fields the same as forested parks.

Our method of identifying open space relies on crowdsourced OpenStreetMap data. We could not verify each asset's quality or availability to the public, so this indicator might overestimate access to open space.

ACC-8: proximity to schools

DEFINITION

The percentage of the population living within a 400 m walk, 15-minute walk (1,125 m), or 15-minute bicycle ride (3 km) of a school.

IMPORTANCE

Proximity to schools is an important indicator of the accessibility of education and other social services for children, and equitable access to schools drives equitable social and economic opportunity more generally (Joshi 2017). SDGs 4.1 and 4.2 call for equitable access to high-quality pre-primary, primary, and secondary education. This indicator considers all kindergartens and primary and secondary schools within walking distance of a city's resident children. Rodríguez-López et al. (2017) found that, on average, urban children tend to use modes of transportation other than walking when schools are more than 1,250 m from their homes.

METHODS

For school locations, we queried OSM for *school* in the building category and *school* and *kindergarten* in the amenity category. We used the point locations of the schools as the focal points of an isodistance analysis as in ACC-6. We estimated travel distances for a given network of streets and roads, which we obtained from OSM. The population within the isochrone and isodistance areas was calculated and then converted to a percentage by dividing that value by the total population of the area of interest. The main population of interest is children, or persons aged 0–14 years. However, accessibility of school to the entire population, to residents of informal settlements, or to children residing in informal settlements might also be of interest. Isochrone calculations using modes of transportation other than walking are contemplated as a future update. We calculated this indicator using the citywide population of children, as well as the subset of children estimated to be living in informal developments, as in ACC-3.

We determined walking time using a walking speed of 4.5 km/hour, the median walking speed in data collected by Schimpl et al. (2011). For bicycle speed, we used 12 km/hour, which is the default bicycle speed in r5r (Saraiva et al. 2025).

LIMITATIONS

The limitations previously described for OSM and WorldPop data, the Intraurban Land Use dataset, and the r5r isodistance calculations apply to this indicator.

There is currently no consistent descriptor within OSM data to differentiate among levels of school. Countries use different terminology to describe categories of schools that differ by the grades they offer and ages they serve. The only consistent differentiation of educational facilities is between primary or secondary education (i.e., elementary through high schools) and higher education (i.e., colleges and universities).

ACC-9: proximity to goods and services

DEFINITION

The percentage of the population living within a 400 m walk, 15-minute walk (1,125 m), or 15-minute (3 km) bicycle ride of buildings used for commercial activity, including stores, shopping centers, supermarkets, and restaurants.

IMPORTANCE

Urban residents must have safe, sustainable, and equitable access to sites where goods and services are bought and sold. This indicator is in alignment with the concept of the 15-minute city (Moreno et al. 2021) and considers all sites of commercial activity within a 15-minute walk or bicycle trip of a city's residences.

METHODS

For places where goods and services are sold, we queried OSM for key-value pairs[8] specified as *commerce* in Table A-1, Appendix A. These included buildings, land parcels, and point locations mapped as banks, shops, cafés, fast food, and veterinary offices.

We used the point locations of these sites as the focal points of an isochrone analysis as in ACC-6. We estimated travel times for a given network of streets and roads, which we obtained from OSM. We calculated the population within 400 m isodistance areas and 15-minute walking and bicycling isochrone areas in r5r or r5py and then converted the value to a percentage by dividing that value by the total population of the area of interest. We conducted these analyses with the total population, women and girls, children, elderly persons, and residents of informal settlements.

We determined walking time using a walking speed of 4.5 km/hour, the median walking speed in data collected by Schimpl et al. (2011). For bicycle speed, we used 12 km/hour, which is the default bicycle speed in r5r (Saraiva et al. 2025).

LIMITATIONS

The limitations previously described for OSM and WorldPop data, the Intraurban Land Use dataset, and the r5r isochrone calculations apply to this indicator.

Regarding the use of walking and bicycling speeds to calculate isochrones, our use of a single representative speed for all calculations does not allow our analyses to reflect the variation in travel times and of isochrone extent that arise from differences in topography, traffic patterns, road and sidewalk conditions, traveler age and health, weather, and numerous other factors that affect travelers' experiences on particular routes.

Because of practical limitations, we treated all goods and services as a single type. That is, we did not differentiate among banks, shops, or cafés, among others. Commercial entities of different types often cluster together in commercial neighborhoods, but not always. This indicator addresses proximity to *any* commercial entity, not proximity to the full range of commercial activities available in a city.

ACC-10: proximity to potential employment

DEFINITION

The percentage of the population living within a 400 m walk, 15-minute walk (1,125 m), or 15-minute (3 km) bicycle ride of sites of commercial or industrial activity, including stores, shopping centers, supermarkets, offices, schools, and factories.

IMPORTANCE

Urban residents must have safe, sustainable, and equitable access to jobs and sites where they can find employment. Employment is an essential urban amenity in the ideal 15-minute city, in which opportunities for work, among other essential social functions, exist within easy access by foot or bicycle (Moreno et al. 2021). This indicator considers all sites of commercial and industrial activity within a 15-minute walk or bicycle trip of a city's residences.

METHODS

We queried OSM for all key-value pairs specified in Appendix A, including all categories of potential employer: *commerce*, *education*, *health care and social services*, *agriculture*, *government*, *industry*, and *transportation and logistics*. These included point locations mapped as banks, shops, cafés, fast food, and veterinary offices.

Isochrones were calculated, and the percentage of the population within 400 m or a 15-minute walk or bicycle ride of at least one potential employer is reported separately for each employer category. We determined walking time using a walking speed of 4.5 km/hour, the median walking speed in data collected by Schimpl et al. (2011). For bicycle speed, we used 12 km/hour, which is the default bicycle speed in r5r (Saraiva et al. 2025).

The point locations of these sites were used as the focal points of an isochrone analysis as in ACC-6. We estimated travel times for a given network of streets and roads, which we obtained from OSM. The population within 15-minute walking and bicycling isochrone areas was calculated in r5r and then converted to a percentage by dividing that value by the total population of the area of interest.

As with ACC-3, we also calculated this indicator using population disaggregated by sex and age class, and by informality of residential settlement.

LIMITATIONS

The limitations previously described for OSM, WorldPop data, the Intraurban Land Use dataset, and the r5r isochrone calculations apply to this indicator.

We considered only potential employers. We were unable to consider whether employers have vacancies, whether available vacancies are well suited to residents within the isochrones, or the quality of the jobs. This analysis also considered employment only at physical, formal business establishments and as a result didn't consider informal employment or remote employment opportunities.

ACC-11: number of potential employers in proximity

DEFINITION

The population-weighted average number of sites of public, commercial, or industrial activity, including stores, shopping centers, supermarkets, offices, schools, and factories that are within a 400 m walk, 15-minute walk (1,125 m), or 15-minute (3 km) bicycle ride of each location in the city.

IMPORTANCE

Indicator ACC-10 reflects the proximity to each resident of *at least one* potential employer. It does not reflect how many potential employers are nearby and therefore addresses the spatial distribution, rather than the volume, of economic activity. Indicator ACC-11 reflects the volume of economic activity, and hence potential employment, conveniently accessible to city residents by walking or bicycling. It is weighted by population, so it reflects the experience of an average city resident.

METHODS

As in ACC-10, we retrieved locations of economic activity, using all categories in Appendix A, from OSM. We considered points that were within 0.0001 degrees of each other (approximately 11 m) duplicates; all but one duplicate were removed. (Note that duplicate points are not a problem for ACC-10.) We calculated 15-minute walking and bicycling isochrones using r5r. Some of these isochrones overlapped. We calculated a raster, each pixel of which stores the number of isochrones that intersect with the pixel center, generating a count of potential employers accessible from that location. To calculate the population-weighted average, we multiplied each pixel value by the fraction of the total population that resides in the area represented by that pixel. Pixels are equal in area, so the indicator is the mean pixel value within the city or district.

We determined walking time using a walking speed of 4.5 km/hour, the median walking speed in data collected by Schimpl et al. (2011). For bicycle speed, we used 12 km/hour, which is the default bicycle speed in r5r (Saraiva et al. 2025).

As with ACC-3, we also calculated this indicator using population disaggregated by sex and age class, and by informality of residential settlement.

LIMITATIONS

The limitations previously described for OSM and WorldPop data, the Intraurban Land Use dataset, the r5r isochrone calculations, and the challenges of using OSM data to represent potential jobs apply to this indicator.

Our method of removing duplicates might have removed records of genuinely separate businesses that appeared to occupy the same location. This error could occur due to human error on behalf of the OSM mapper, because the locations are closer together than 0.0001 degrees, or because one of the businesses is directly above the other in a multilevel building. This indicator might underestimate the density of potential employers, especially in dense cities. Removing duplicates is a conceptual and technical challenge, and improving our method of doing so is a priority for future work.

This indicator does not consider the quality, availability, or number of jobs at sites identified as potential employers.

ACC-12: proximity to public transportation

DEFINITION

The percentage of the population living within a 500 m walk, 15-minute walk (1,125 m), or 15-minute (3 km) bicycle ride of a public bus, tram, trolley, subway, train, ferry, or aerialway stop.

IMPORTANCE

Equitable access to public transportation allows a city's residents more sustainable and equitable access to a greater quantity and variety of economic, social, and recreational amenities. This indicator directly supports Global Urban Monitoring Framework Indicator 1.2.2 and SDG Indicator 11.2.1, which measure a population's convenient access to public transportation. UN-Habitat considers a transit stop to be conveniently accessible if it is within a 500 m walk (UN-Habitat 2018, 2022). Because a 500 m isodistance area is similar to a 400 m isodistance area, we did not calculate this indicator using a 400 m isodistance area.

METHODS

For transit stop locations, we queried OSM for the following:

- *Ferry terminal* in the amenity category
- *Stop*, *platform*, *halt*, *tram stop*, *subway entrance*, and *station* in the railway category
- *Bus stop* and *platform* in the highway category
- *Platform*, *stop position*, and *stop area* in the public transport category
- *Subway* in the station category
- *Station* in the aerialway category

We used the point locations of these sites as the focal points of an isochrone analysis as in ACC-6. We estimated travel times for a given network of streets and roads, which we obtained from OSM. Population estimates are from WorldPop unconstrained 100 m gridded population estimates. The population within the isochrone or isodistance area was calculated and then converted to a percentage by dividing that value by the total population of the area of interest. We conducted these analyses with the total population, women and girls, children, elderly persons, and residents of informal settlements.

Walking time was determined using a walking speed of 4.5 km/hour, the median walking speed in data collected by Schimpl et al. (2011). For bicycle speed, we used 12 km/hour, which is the default bicycle speed in r5r (Saraiva et al. 2025).

LIMITATIONS

The limitations previously described for OSM data, WorldPop's unconstrained population estimates, assessment of informality in the Intraurban Land Use dataset, and the r5r isodistance calculations apply to this indicator. In addition, we did not have global access to data on the frequency of transit vehicles or the importance of particular stops in terms of route popularity or connectivity. Our method treated all stops as equivalent to one another.

ACC-13: proximity to health care

DEFINITION

The percentage of the population living within a 400 m walk, 15-minute walk (1,125 m), or 15-minute (3 km) bicycle ride of a hospital, clinic, or doctor's office.

IMPORTANCE

Reducing travel distance to hospitals is associated with improved health outcomes, including outcomes in cardiac crises and unintentional injuries (Buchmueller et al. 2006), maternal and perinatal outcomes from childbirth (Minion et al. 2022), and preventative care (Dai 2010). This indicator supports assessment of the spatial accessibility of hospitals, clinics, and doctors' offices.

METHODS

For health care facility locations, we queried OSM for the following:

- *Doctors* and *hospital* in the amenity category
- *Clinic* and *hospital* in the building category

We used the point locations of these sites as the focal points of an isochrone or isodistance analysis as in ACC-6. We estimated isochrone and isodistance polgygons for a given network of streets and roads, which we obtained from OSM. We retrieved population estimates from WorldPop unconstrained 100 m gridded population estimates. The 400 m distance threshold aligns with Global Urban Monitoring Framework Indicator 1.2.1 (UN-Habitat 2022). We calculated the population within the isochrone or isodistance areas and then converted that value to a percentage by dividing it by the total population of the area of interest. We conducted these analyses with the total population, women and girls, children, elderly persons, and residents of informal settlements.

We determined walking time using a walking speed of 4.5 km/hour, the median walking speed in data collected by Schimpl et al. (2011). For bicycle speed, we used 12 km/hour, which is the default bicycle speed in r5r (Saraiva et al. 2025).

LIMITATIONS

The limitations previously described for OSM data, WorldPop's unconstrained population estimates, the Intraurban Land Use dataset, and the r5r and r5py isodistance calculations apply to this indicator.

This analysis treats hospitals, clinics, and doctors' offices as equivalent, despite the large differences in capacity among these types of health care facilities.

Air quality (AQ)

Air quality is a major factor in the physical health of urban residents. Cities both produce air pollution and are impacted by pollution. These indicators measure city contributions to air pollution and resident exposure to pollution. Higher values are associated with greater hazard, exposure, or vulnerability.

AQ-1: air pollutant emissions

DEFINITION

The annual air pollutant emissions from city areas (tonnes) and related social costs (in US dollars), disaggregated by pollutant and sector.

IMPORTANCE

Human activity contributes to air pollution and climate change through greenhouse gas emissions from fuel combustion, industrial processes, and agriculture. This pollution imposes social costs through its negative impacts on human health and economic productivity. This indicator can help decision-makers and stakeholders identify the most important pollutants emitted locally, the activities responsible for the emissions, and, with multiple years of data, understand emissions trends over time.

METHODS

This indicator is based on the Global Anthropogenic Emissions dataset of the Copernicus Atmosphere Monitoring Service (CAMS) and the Emissions of atmospheric Compounds and Compilation of Ancillary Data (ECCAD) (Granier et al. 2019).[9] The dataset provides annual estimates of emissions from 12 sectors of human activity, on a 0.1-degree (approximately 11 km) spatial resolution. The estimates are based on simulations and historical data and are updated intermittently. The included sectors are agriculture (livestock); agriculture (soils); agriculture (waste burning); power generation; fugitive emissions; industry; combustion in residential, commercial, and other settings; ships; solvents; solid waste and wastewater; off-road transportation; and on-road transportation.

We used Google Earth Engine to calculate the emissions from within our areas of interest (city administrative boundaries). We extracted annual, sector-disaggregated emissions in tonnes per year for each of the health-related pollutant species available in the dataset: black carbon (BC), methane (CH_4), carbon monoxide (CO), nitrogen oxides (NO_x), sulfur dioxide (SO_2), organic carbon (OC) compounds, ammonia (NH_3), and non-methane volatile organic compounds (NMVOCs). Because of the coarse resolution of this dataset, we report values for the geographic area of only the full city and not for each subcity area.

LIMITATIONS

The emissions data used for this indicator account for only direct emissions from activities within the boundaries of the city (Scope 1 emissions). They do not account for emissions associated with electricity that is used in the city but generated elsewhere (Scope 2); or emissions produced elsewhere associated with products or services consumed in the city (Scope 3), such as air pollution from fires in formerly forested areas cleared to produce agricultural commodities consumed in cities, including beef and palm oil. Additionally, this analysis does not provide information on where the social cost of these emissions accrues. Because pollution travels and most costs are associated with pollution exposure, not emissions, many of the costs associated with pollution from the city may be experienced outside the city.

The CAMS dataset is modeled data based on an ensemble of multiple emissions models and is subject to the limitations of those models. The methods used to develop the CAMS emissions dataset are described in Granier et al. (2019).

Some audiences might be accustomed to seeing pollutant concentrations reported on a per-capita or per-area basis. After conducting additional research into our target users' preferences, we might change our reporting of this indicator to a per-capita or per-area basis.

AQ-2: social cost of air pollution

DEFINITION

The estimated cost to society of air pollution, in US dollars per year.

IMPORTANCE

AQ-1 reports air pollution in terms of pollutant concentration, but concentrations can be difficult to interpret. This indicator expresses the information in AQ-1 in terms of estimated monetary cost to society of the health damage caused by air pollution. The social cost can be used for cost-benefit analyses and to communicate the urgency of air quality interventions.

Table 1 | **Estimated social cost for each pollutant species**

POLLUTANT SPECIES	SOCIAL COST PER TONNE (US$)
Ammonia (NH_3)	22,000[a]
Black carbon (BC)	62,000[a]
Carbon dioxide (CO_2)	0[a]
Carbon monoxide (CO)	250[a]
Methane (CH_4)	740[a]
Nitrogen oxides (NO_x)	67,000[a]
Non-methane volatile organic compounds (NMVOCs)	1,172[b]
Organic carbon (OC)	51,000[a]
Sulfur dioxide (SO_2)	33,000[a]

Notes: a Nonclimate health-related costs are estimated in Shindell (2015). b The median cost across four German regions for emissions below 100 meters, as estimated in van der Kamp (2017).

Source: WRI authors.

METHODS

We converted tonnes of pollutant from AQ-1 to US dollars based on health-related social costs per tonne (Table 1) as estimated by Shindell (2015) for all pollutant species except NMVOCs. For the social cost of NMVOCs, we used the median value for NMVOCs emitted below an elevation of 100 m in van der Kamp (2017). Van der Kamp's estimates are in 2015 €, which we converted to 2015 US$ at €1 = $1.11. We report annual emissions and social costs as a time series for the years 2000–24. Provision of future years' data will depend on the availability of updates to the CAMS data.

We summed the daily cost for each pollutant species over the year in question and report the annual sum.

LIMITATIONS

The limitations of our method of estimating pollutant concentrations in AQ-1 apply to this indicator. In addition, our simple method of converting concentrations to social cost ignore enormous complexities in atmospheric mixing, health impacts, the societal cost of health impacts, and the values of currencies relative to the US dollar. The estimates we provide based on global data should not be used in place of local studies using local data and assumptions.

AQ-3: high pollution days

DEFINITION

The annual number of days that air pollutants were above World Health Organization (WHO) air quality standards in the year of interest.

IMPORTANCE

Exposure to high concentrations of air pollutants increases the probability of developing serious health conditions, reduced lung function, increased susceptibility to respiratory infections, and aggravated asthma. Long-term exposure increases the probability of developing chronic conditions such as stroke susceptibility, heart disease, and cancer (Kampa and Castanas 2008; Lee et al. 2018). This indicator can help public health officials determine which air pollutants are present at levels dangerous to human health and how many days each year the population is exposed to them.

METHODS

The data used for this indicator come from the CAMS Global Reanalysis EAC4 dataset (Inness et al. 2019), which combines satellite monitoring of pollutant concentrations with atmospheric modeling to estimate concentrations near the Earth's surface.[10] The EAC4 data are provided at an approximately 80

Table 2 | **WHO standards for outdoor air pollutants**

POLLUTANT SPECIES	AVERAGING TIME (HOURS)[A]	WHO-RECOMMENDED AIR QUALITY GUIDELINE MAXIMUM LEVEL
Carbon monoxide (CO)	24	4,000 µg/m^3
Coarse particulate matter (PM_{10})	24	45 µg/m^3
Fine particulate matter ($PM_{2.5}$)	24	15 µg/m^3
Nitrogen dioxide (NO_2)	24	25 µg/m^3
Ozone (O_3)	8[b]	100 µg/m^3
Sulfur dioxide (SO_2)	24	40 µg/m^3

Notes: Abbreviations: WHO = World Health Organization; µg/m^3 = micrograms per cubic meter; $PM_{2.5}$ = particulate matter of 2.5 micrometers or less in diameter; PM_{10} = particulate matter of 10 micrometers or less in diameter. [a] The WHO provides additional guidelines for the same pollutants for other averaging times. [b] Due to limitations with the Copernicus Atmosphere Monitoring Service dataset, for the ozone calculations, we used data for the nine-hour window of 6 a.m. to 3 p.m. In some parts of the world, the highest level of ozone is reached after 5 p.m.

Source: WHO 2021.

km spatial resolution. Because of the coarse resolution of this dataset, we report values for the geographic area of only the full city and not for each subcity area.

We report the number of days each city was estimated in the year of interest to have had a near-surface concentration of air pollutants that exceeded WHO's standards for outdoor air pollutants (WHO 2021). The indicator is reported as a time series of annual values. Table 2 outlines the pollutants and standards used.

LIMITATIONS

The CAMS data have uncertainty related to the limitations of the atmospheric modeling methods used. Additionally, the low resolution of the dataset does not allow for analysis of subcity geographic units and may introduce uncertainty to the city-scale calculations due to aggregated data from an area larger than the city.

AQ-4: exposure to fine particulate matter

DEFINITION

The population-weighted annual mean fine particulate matter ($PM_{2.5}$) concentration as a percentage of the WHO's air quality guideline for annual exposure.

IMPORTANCE

$PM_{2.5}$ consists of very small particles with diameters of 2.5 micrometers (µm) or less. (For comparison, a typical human hair has a diameter of 50–70 µm.) $PM_{2.5}$ is released from combustion (including fuel combustion in vehicles and power plants, the use of wood and other biomass for cooking and heating, as well as wildfires), degradation of vehicle tires during use, and some chemical processes that occur in the atmosphere. $PM_{2.5}$ is a serious health concern because the small size allows $PM_{2.5}$ particles to travel deep into human lungs, enter the bloodstream, and cause direct damage to internal organs. Long-term exposure to $PM_{2.5}$ leads to increased incidence of heart and lung diseases, cancers, and premature death (Feng et al. 2016; WHO 2021). This indicator can help decision-makers determine how many city residents face long-term exposure to dangerous levels of $PM_{2.5}$ and in which neighborhoods these residents live.

METHODS

For this indicator, we used the global surface PM2.5 V5. GL.02 dataset from the Atmospheric Composition Analysis Group at Washington University in St. Louis (van Donkelaar et al. 2021).[11] This dataset combines models of atmospheric mixing and chemistry with analysis of imagery from the Moderate Resolution Imaging Spectroradiometer, Multi-angle Imaging SpectroRadiometer, and Sea-viewing Wide Field-of-view Sensor satellite instruments from the National Aeronautics and Space Administration (NASA) to generate estimates of $PM_{2.5}$ concentrations near the Earth's surface. The data are provided at a spatial resolution of 0.01 degrees, or approximately 1.1 km.

For each year of interest, we found the average $PM_{2.5}$ concentration for each 0.01-degree pixel within the city boundary, and weighed it by the fraction of the total population that was found within that pixel. Population data are the 2020 unconstrained estimates from WorldPop. We report the population-weighted concentration as a percentage of the WHO's air quality guideline (recommended maximum level) for annual exposure: 5 µg

per cubic meter (m^3) (WHO 2021). We calculated the annual average spatially over the area of the district. For example, an average concentration of 15 $\mu g/m^3$ would be reported as 300 percent of the WHO standard. This indicator is based on the WHO annual average concentration recommendation for $PM_{2.5}$, as distinct from the WHO 24-hour average recommendation used in indicator AQ-3. We report this indicator as a time series for the years 2000–22. Provision of future years will depend on the availability of updates to the source dataset. We report time series for the general population as well as for children, elderly residents, female residents, and residents of areas with informal development.

LIMITATIONS

The $PM_{2.5}$ dataset has uncertainty related to the limitations of the atmospheric modeling methods that it uses. The concentration levels we report cannot be directly translated into health impacts. The health impacts of air pollution are not linearly related to pollutant concentrations, so although higher concentrations are worse for health, concentrations at, for example, 300 percent of the WHO standard should not be interpreted as being three times worse than concentrations at 100 percent.

If this indicator is reported only at an all-city level, basing this indicator on an all-city average might obscure pollution hotspots. For all-city reporting, it might be useful to consider reporting the maximum exposure rather than the average. We report this indicator at the all-city level as well as for subcity administrative districts.

Biodiversity (BIO)

Cities are often thought of as detrimental to biodiversity—and they can have significant negative impacts related to habitat loss and resource extraction—but cities can also make choices that mitigate biodiversity loss and enhance habitat.

Most of the indicator methods in this category are based on the indicator definitions used in the Singapore Index on Cities' Biodiversity (Chan et al. 2021) and the IUCN Urban Nature Indexes (IUCN 2023). Both are widely recognized assessment frameworks designed to help assess and track biodiversity and its protection within cities. They encompass assessment of biodiversity, access to the societal benefits of biodiversity, and government structures and processes supporting biodiversity. They can be used to assess the status of local biodiversity and the conditions that support it as well as identify priority areas for future urban biodiversity efforts.

The indexes define indicators and scoring methods, and cities are invited to adapt the indicators and definitions for their own purposes. The indexes do not provide data for calculating indicator values, and data acquisition and processing can pose challenges for some cities. We provide data supporting a subset of the Singapore Index's and UNI's indicators that address biodiversity and access to benefits. Some of the biodiversity indicators do not measure biodiversity directly but rather conditions that support or harm biodiversity. We have defined and implemented our indicators to adhere as closely as possible to the definitions in the Singapore Index. Our approach prioritizes global, publicly available, and peer-reviewed datasets to develop indicators; however, cities often have access to local data that are of higher quality or are more specifically suited to local contexts and needs.

For these indicators, higher values are associated with greater biodiversity or greater support for biodiversity.

BIO-1: natural areas

DEFINITION

The percentage of land that is within natural area land classes.

IMPORTANCE

Natural areas support biodiversity by providing habitat. They also provide human beings with ecosystem services. The portion of the total city area that is close to a natural state thus gives information about a city's biodiversity and about the benefits provided by biodiversity.

METHODS

Natural ecosystems, as defined by the Singapore Index, are all areas that are not highly disturbed or completely human altered. Examples of natural ecosystems include forests, mangroves, freshwater swamps, natural grasslands, streams, and lakes. We calculated this indicator as the percentage of natural area within the city boundary:

$$100\% \times \frac{\text{total natural area}}{\text{area of city}}$$

We calculated this indicator using the ESA WorldCover 10 m 2021 V200 land-classification map (Zanaga et al. 2021). We included as natural area all land classified in this dataset as trees, shrubland, grassland, herbaceous wetland, mangrove, or moss and lichen.

LIMITATIONS

- The ESA WorldCover 10 m 2020 V100 layer was assessed to have overall accuracy of 74.4 percent (Tsendbazar et al. 2021). The dataset we used, being similar to the V100 dataset, is therefore very likely to include errors in land cover classification. These errors would be carried through to our characterization of natural and nonnatural lands.
- The WorldCover dataset has a spatial resolution of 10 m. For some wildlife species, patches smaller than 10 m might provide useful habitat. WorldCover and our implementation of this indicator could fail to account for these tiny patches.
- Some species have requirements with respect to habitat patch size, plant-community composition, level of vegetation homogeneity, and composition of nearby land. Our method accounts for none of these (or other) potentially important ecological details. Biodiversity planning that prioritizes particular species or that is informed by a locally implemented ecological assessment should contemplate augmenting our indicators with local ground truthing and habitat classifications defined by local species' requirements.
- For many biodiversity-planning purposes, highly managed grassy areas such as lawns and golf courses might not be considered natural. However, as WorldCover classifies these areas as grass, our method classifies them as natural area.

BIO-2 and BIO-3: connectivity of natural lands

DEFINITION

Landscape coherence (BIO-2) and effective habitat mesh size (BIO-3) are measures of the connectivity of patches of land that can serve as habitat for wild animals. Values for both range from 0 to 1, with larger values indicating greater ease of animal movement between habitat patches.

IMPORTANCE

In general, contiguous habitat benefits biodiversity better than habitat that is subdivided by roads, buildings, and other built infrastructure (Forman and Godron 1991; Fahrig 2003). The connectivity of habitat patches mitigates the effects of habitat fragmentation by allowing wildlife to access more habitat without having to cross inhospitable terrain. The fragmentation of natural areas affects species differently. For example, a road might not be a barrier for birds, but it can seriously fragment a population of arboreal primates. Although consideration of dispersal ability and habitat requirements are important in the management of particular species, the Singapore Index adopts a generalist approach to quantifying connectivity based purely on patch geometry.

Indicator 3.5 of the IUCN Urban Nature Indexes uses effective mesh size as a measure of habitat connectivity (IUCN 2023). Indicator 2 of the Singapore Index uses landscape coherence (Chan et al. 2021). We calculated both.

PLAIN-LANGUAGE CONCEPTUAL DEFINITIONS

A **natural area** is land that is hospitable to wild animals. Because animal species differ in their habitat requirements, the concept of a natural area is necessarily nonspecific and is taken by the Singapore Index and by us to encompass natural, near-natural, and other lands that are relatively undisturbed by human activity.

Connected natural area patches are patches that are separated from each other at their nearest points by 100 m at most. Most animals can move from one habitat patch to another, crossing some distance of inhospitable land. Animal species differ in their movement behaviors and their tolerance of nonhabitat environments, so the Singapore Index uses a generally useful distance to define patch isolation. The 100 m threshold was chosen by a consensus of expert advisers to the Singapore Index.

Effective mesh size and coherence are landscape measures of natural area connectivity. **Effective mesh size (EMS)** is the probability that any two randomly selected points in a city's natural areas will be located in the same contiguous natural area patch, or network of connected patches. If the two random points represent the locations of two animals of the same species, the EMS models the probability that they encounter one another. EMS is the sum of the squared areas of each natural area patch, divided by the total natural area. (The areas of patches that are connected to each other are summed and treated as a single patch.) Maximum EMS would indicate a landscape in which all natural area exists as a single contiguous (or connected) patch: Coherence would be unity. A landscape in which natural area is subdivided into many isolated patches would have coherence between 0 and unity. **Coherence** is the EMS divided by the total natural area. This normalizes the EMS to be between 0 and 1, so that coherence is the sum of squared areas of each natural patch, divided by the squared total natural area. Because it accounts for the variation in area among cities, it is useful for among-city comparisons.

METHODS

We calculated this indicator using the ESA WorldCover 10 m 2020 V100 land-classification map (Zanaga et al. 2021). We included as natural area all land classified as trees, shrubland, grassland, herbaceous wetland, mangrove, or moss and lichen.

We calculated the EMS (BIO-3) using the following equation:

$$EMS = \frac{1}{A_{total}}(A_{G1}^2 + A_{G2}^2 + \cdots + A_{Gn}^2)$$

where A_{total} is the total area of all natural areas; A_{G1} to A_{Gn} are the sizes of each group of connected patches of natural area that are distinct from each other; and n is the total number of groups of connected patches of natural area. A_{G1} to A_{Gn} may consist of areas that are the sum of two or more smaller patches that are connected. In general, patches were considered to be connected if they were less than 100 m apart. We derived this equation from Deslauriers et al. (2018).

We calculated coherence (BIO-2) as $coherence = EMS / A_{total}$.

LIMITATIONS

- This indicator shares the limitations of BIO-1, which stem from unavoidable errors in land classification.
- This indicator does not currently address roadways as particular dangers to animals, despite the well-documented role that vehicle collisions play in harming wildlife (Sugiarto 2022). We would like to integrate roadway information into our implementation of future versions of this indicator.
- We considered two habitat patches to be connected if they were no more than 100 m apart. We took the 100 m threshold from the definition of the corresponding indicator in the Singapore Index, but its appearance there does not suggest any universal applicability to all types of animal movement. Some flying animals are likely to tolerate greater distances, and some small animals (especially amphibians) cannot traverse 100 m of, say, pavement. Biodiversity planning that prioritizes certain animals for protection should contemplate implementing this indicator using a distance threshold that accounts for the specific movement behaviors and physiological tolerances of the species of interest.

BIO-4: biodiversity in built-up areas (birds)

DEFINITION

The percentage of bird species in all areas that were also observed in built-up areas.

IMPORTANCE

Cities often include large amounts of built-up and denuded land. These areas are not typically thought of as high-quality habitat, but they can support some species. This indicator reflects the ability of built-up areas to support biodiversity, using birds as an indicator group. Built-up areas include impermeable surfaces such as buildings, roads, and drainage channels as well as anthropogenic green spaces such as roof gardens, roadside plantings, golf courses, private gardens, cemeteries, lawns, and urban parks.

METHODS

We calculated the indicator using the following equation:

$$100\% \times \frac{\text{number of bird species observed in built up areas}}{\text{number of bird species observed in all areas of city}}$$

To delineate built-up areas, we used the ESA WorldCover 2021 classification of built-up land (Zanaga et al. 2021). For the number of bird species, we estimated the saturation levels of species-area curves as described for indicators BIO-4, BIO-5, and BIO-6, using research-grade observations of birds over a five-year period in the crowdsourced iNaturalist database, accessed through the Global Biodiversity Information Facility (GBIF 2025). Calculations were made using only the observations that occurred on built-up land and using all observations within city boundaries. We report the built-up estimate divided by the all-city estimate.

LIMITATIONS

This method shares the limitations of BIO-4, BIO-5, and BIO-6, as well as the following:

- The WorldCover dataset's built-up classification is subject to error due to both automated data processing and resolution issues.
- All estimates include unavoidable errors. This indicator is calculated from two estimates, and so the potential error is greater. When nearly the entire city or district is built up, the estimated species count on built-up land will be very similar to the citywide estimate, and the indicator value will be close to 1. Occasionally, the calculated value is greater than 1 because of errors introduced by the methods used to produce the numerator, the denominator, or both. In these cases, because values greater than 1 are impossible, we report the value as 1.

Because this indicator requires several years of data to calculate, and because high-quality iNaturalist data have only recently become available, it is not yet possible to provide this indicator as a time series. As iNaturalist data continue to be updated, we expect to be able to report estimates for more than one time point for comparison.

BIO-5–BIO-7: number of vascular plant, bird, and arthropod species

DEFINITION

The estimated number of vascular plant (BIO-5), bird (BIO-6), and arthropod (BIO-7) species over a five-year period.

IMPORTANCE

Direct measurement of biodiversity is important, but it would be impossible to directly assess the diversity and health of all wild populations in a city. We therefore provide species-richness data for the three indicator taxa chosen by the Singapore Index as proxies for overall biodiversity: vascular plants, birds, and arthropods. The change in species richness for these major groups is likely to be directly associated with changes in general habitat quality and in overall biodiversity.

- Vascular plants are plants with vascular tissues, which conduct water, minerals, and the products of photosynthesis throughout the plant. In contrast to nonvascular plants (e.g., mosses), vascular plants can grow tall and in locations with little moisture on the surface of the soil. Vascular plants include more than 90 percent of the Earth's vegetation.
- Birds are one of the most visible species groups in urban areas, and they are often considered a key indicator of environmental quality. They are well studied by professional and amateur naturalists worldwide, are sensitive to environmental and habitat changes, and are comparatively easy to observe and count. The Singapore Index includes the change in the number of bird species over time.
- Arthropods include insects, spiders, crustaceans, and other animals with exoskeletons and jointed limbs. They are important actors in terrestrial ecosystems, driving critical processes such as pollination, food-web relations, and nutrient cycling. Many are highly sensitive to changes in their physical and ecological environments.

The Singapore Index recommends reporting the number of native species in each of these groups in regular time intervals. A local data collection process would typically involve partnering with a local research institution to carry out a species survey. This survey would be repeated every few years; the indicator is the change in time from a baseline level to the current year. Here, we provide species counts estimated from crowdsourced species-occurrence datasets. Our method cannot substitute for on-the-ground species surveys. We intend it to provide rough estimates that can be used in the absence of more intensive efforts.

Figure 3 | **An example of a species accumulation curve**

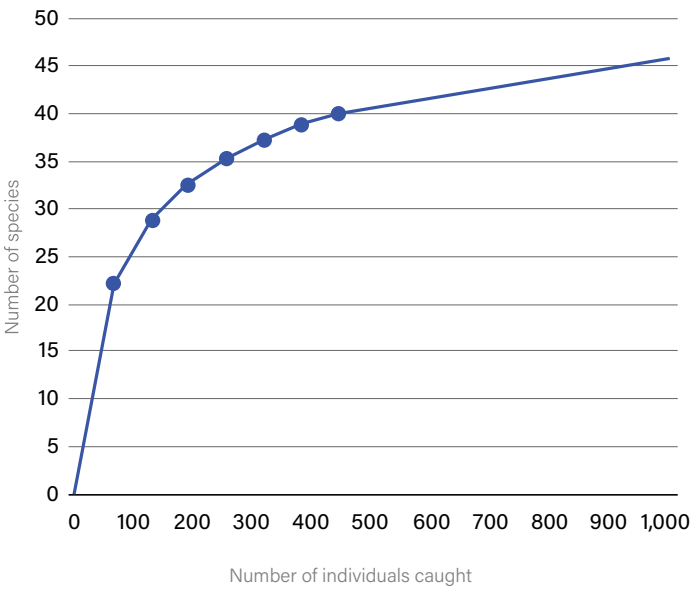

Note: In a field species census, as more individuals are caught, the more unique species are identified. Because the addition of unique species grows more slowly at high capture numbers, it is possible to extrapolate the curve and estimate a saturation species number.

Source: Terrestrial Ecosystems n.d.

These indicators support Singapore Index Indicators 4–6 and IUCN Urban Nature Indexes Indicators 4.1 and 4.2.

METHOD FOR ESTIMATING SPECIES NUMBER

Biologists often interpret species survey data by examining the number of species found as a function of effort, plotted as a species accumulation curve (SAC). The SAC plots the cumulative number of species recorded as a function of sampling effort (i.e., number of individuals collected or cumulative number of samples). At the start of a species survey, the total number of species found typically grows quickly with every unit of effort. After some time, however, effort expended yields more and more species that were found earlier in the survey—and the total number of species grows more slowly per unit of effort. A plot of species number versus effort will come to a plateau, and this saturation level is a common estimator for the number of species in an area, as shown in Figure 3.

We estimated species richness by estimating the saturation level of SACs using individual crowdsourced observations as our effort unit. The estimated counts are the mean saturation levels of 100 SACs, each generated by randomizing the order of all research-grade iNaturalist observations of the *Aves* (birds), *Tracheophyta* (vascular plants), and *Arthropoda* (arthropods) taxa (GBIF 2025) in 2019–24. Only species observations with enough data to generate SACs were considered for estimating species richness. Although using just one year of observations might have allowed us to associate species count estimates with particular years, observation data in most cities were insufficient when we limited our method to single-year data. We thus combined data over six years to increase the number of cities for which we could report estimates.

LIMITATIONS

We used the SAC curve-fitting approach because it was impossible to conduct an exhaustive survey of all species present even in the indicator taxa. However, our reliance on crowdsourced species observations introduces serious limitations:

- Citizen-scientist observations do not benefit from deliberate spatial sampling techniques. One consequence is that the observations that informed our calculations tended to be clustered in heavily populated areas and popular recreational sites. We are therefore likely to have missed species that tend to avoid human activity. This probably biases our estimates toward undercounts. See DiCecco et al. (2021) and Grande et al. (2022) for detailed treatments of the issues with crowdsourced biodiversity data.
- Our curve-fitting method included a step that randomized the sequence in which observations were incorporated into the SAC. Because of the randomization, calculating any of these indicators twice with the same data generally yields slightly different values. We tried to minimize the randomization effects by averaging over 100 instances of the curve-fitting step, but we were unable to eliminate the effect entirely.
- In many cities and subcity areas, there were not enough citizen-scientist observations to estimate a plausible SAC. This can be true for any number of the indicator taxa. When there were insufficient data, we were unable to report a species count estimate.
- We were unable to distinguish between native and introduced species. Our estimates almost certainly include introduced species, and in this way our indicators differ from their counterparts in the Singapore Index. Introduced species can (but do not always) harm native populations and ecosystems, and so a large species count—if it does not exclude introduced species—should not be taken as an unambiguous signal of good ecological health.

Because these indicators require several years of data to calculate, and because high-quality iNaturalist data have only recently become available, it is not yet possible to provide these indicators as a time series. As iNaturalist data continue to be updated, we expect to be able to report estimates for more than one time point for comparison.

Flooding (FLD)

Most cities are sited based on access to water for use in agriculture, power, transportation, or other purposes. But proximity to water also exposes cities to the risk of flooding, which is expected to increase in most of the world with a changing climate. These indicators measure city exposure to a variety of flood-related risks. For these indicators, higher values are associated with greater hazard, exposure, or vulnerability.

FLD-1: exposure to coastal and riverine flooding

DEFINITION

The percentage of built land exposed to coastal or riverine flooding.

IMPORTANCE

Most cities are built near coasts or along rivers. These natural assets for economic development can also present a hazard when they cause flooding in built-up areas. The prevalence of these floods is increasing globally due to sea-level rise, extreme precipitation, and snowmelt caused by climate change.

METHODS

We used projections from Aqueduct Floods (Ward et al. 2020), with a resolution of 30 arc seconds (approximately 1 km), retrieved through Google Earth Engine to characterize the coastal and riverine flood hazards for each city in terms of meters of expected inundation depth for a given scenario.[12] The scenario variables we used include a 100-year return period (providing the expected depth of inundation from a once-in-100-years flood event), the business-as-usual (Representative Concentration Pathway 8.5) climate scenario, high sea-level rise, no subsidence, and the mean inundation depth from the results of all five riverine projection models that are available in Aqueduct Floods. We then compared locations of either projected coastal or riverine flooding to built-up areas in the city in 2020 as defined by the built-up class from ESA WorldCover. For each city and city district, we calculated the number of built-up

pixels and the number of built-up pixels projected to experience a flood inundation depth greater than zero under the described flooding scenario. Then we calculated the percentage of built-up pixels with flood exposure.

Aqueduct Floods projections are available for the years 2010, 2030, 2050, and 2080. We report this indicator as a time series of values for these years.

LIMITATIONS

The Aqueduct Floods dataset with a 1 km resolution may be too coarse for some applications, including those related to assessing flood risk for individual blocks and buildings. Additionally, because this indicator considers built-up areas in 2020 compared with projected 2030, 2050, and 2080 inundation, it may underestimate built area exposed to the hazard as a result of future land development. Note, however, that this is an indicator of flood hazard, and it does not consider how mitigation measures such as flood protection infrastructure (e.g., levees) may impact the risk of inundation from flooding under the scenario described. This indicator is limited in scope to riverine and coastal flooding hazards, which are modeled independently—combined effects from riverine and coastal floods are not included. It also does not describe hazards from flash pluvial flooding resulting from heavy precipitation events.

FLD-2: expected annual days with extreme precipitation

DEFINITION

The expected annual number of days with one-day precipitation exceeding the local 90th percentile calculated for three 10-year periods: 2020–29, 2040–49, and 2060–69.

IMPORTANCE

Extremely high volumes of one-day precipitation can overwhelm stormwater management systems, particularly as climate change causes some cities to become wetter (Malik and James 2007; Rosenberg et al. 2010). This indicator supports long-term planning for heavy precipitation and can help engineering departments design both gray and green stormwater infrastructure (Bell et al. 2019; van Oorschot et al. 2024).

METHODS

Extreme precipitation for this indicator is defined as the local 90th percentile of cumulative one-day precipitation, calculated for the years 1980–2014 for the pixel that includes the city centroid. The historical data are from the ERA daily reanalysis dataset (Hersbach et al. 2020).

This indicator is the expected value of the number of days during which total precipitation exceeds the 90th percentile. The estimate of the expected value is based on a probability model parameterized using model outputs from the NEX-GDDP-CMIP6 ensemble of downscaled global climate simulations (NASA 2023). We were able to estimate expected values over 10-year future periods, for any decade ending in or before 2100, with simulations using either the SSP2-4.5 or the SSP5-8.5 emissions scenarios[13] (Riahi et al. 2017). Details on the probability modeling are in Wong and Switzer (2023).

The spatial resolution of the NEX-GDDP-CMIP6 climate simulations is 0.25 degrees, or approximately 25 km. This resolution is too coarse to inform most subcity decision-making, so we report this indicator as three numbers for the decade of interest—the estimates from the three NEX-GDDP-CMIP6 models whose historical temperature predictions are closest to the ERA5[14] historical data—estimated at the centroid of the city or district. We currently report this indicator for three decades—2020–29, 2040–49, and 2060–69—using SSP2-4.5.

LIMITATIONS

This indicator is based on estimates of precipitation magnitude probabilities as modeled by climate simulations. There are unavoidable errors—including climate stochasticity, scientific uncertainty regarding Earth system processes, and uncertainty in future greenhouse gas emissions trends—from numerous sources. Notably, we used the expected value of a random variable to capture information about a probability distribution in a single number. It should not be interpreted as a prediction.

Maximum daily precipitation is also not a direct predictor of flooding. It does not account for aggravating or moderating factors such as antecedent rainfall, the local geography of impervious surfaces or stormwater management systems, or topography.

Our method does not distinguish between rain and frozen precipitation.

FLD-3: land near natural drainage

DEFINITION

The percentage of built land cover within 1 m above the nearest drainage.

IMPORTANCE

Land near natural drainage (e.g., streams, rivers) is at risk for pluvial or flash flooding hazards. Development closer in elevation to natural drainage, especially near drainage for large land areas, is at greater risk. The risk for these types of floods

can be difficult to predict, and beyond height above drainage, other factors—such as the amount of precipitation, soil type, extent of impervious surfaces, distance from natural drainage, and presence and efficacy of built drainage systems—are also important influences.

METHODS

For this indicator, we used 30 m resolution data on height above drainage channels from the Global 30m Height Above the Nearest Drainage dataset (Donchyts et al. 2016)[15] to estimate the land area 1 m or less above the nearest drainage for drains with a flow accumulation area of at least 1 square km. We then compared these areas to built-up areas in the city as defined by the built-up class from the ESA WorldCover for 2020.[16] For each city and city district, we calculated at a 10 m scale the number of built-up pixels and the number of built-up pixels within 1 m of the nearest drainage. Then we calculated the percentage of built-up pixels that were 1 m or less above the nearest drainage.

LIMITATIONS

Although this indicator is an important factor related to flash flooding hazards, it does not include other important information (e.g., soil type, artificial drainage systems) essential to comprehensively assessing them. The resulting spatial analysis should not be interpreted as a hazard map. Because it does not incorporate data on artificial drainage networks or the city's conveyance and routing of water (e.g., sewers, drains, canals), this analysis does not provide a comprehensive picture of where water is going and where it is likely to stagnate during pluvial flooding; rather, it provides only an extremely rough approximation.

FLD-4: impervious surface on urbanized land

DEFINITION

The percentage of urbanized land that has impervious surfaces.

IMPORTANCE

Impervious surfaces (in urban areas, these are typically buildings and roads and other pavement) prevent water from soaking into the ground on-site, contribute to decreased overall water infiltration and increased runoff, and can raise the prevalence of localized flooding. This type of flooding also lowers the quality of receiving waters fed by surface water runoff, impacting the biodiversity of aquatic and marine systems downstream. Building cities in ways that minimize impervious surfaces (with alternative construction materials or intentional greening) allows for greater natural water infiltration and can enable cities to "sponge" up excess water, decrease the risk of flooding, and recharge groundwater resources.

METHODS

We obtained the estimated extent of impervious areas from Tsinghua University's annual maps of global artificial impervious area (Gong et al. 2020).[17] This 30 m resolution dataset defines a pixel with at least 50 percent estimated impervious surface as being impervious. We compared the impervious area within the urban extent to the total urban-extent area, using the urban extents dataset from Angel et al. (2024). For each city and city district, we calculated the urbanized area and the area of impervious built-up pixels at a 10 m scale. Then we calculated the percentage of urbanized area that is impervious. This indicator is similar to LND-1, with two distinctions. This indicator considers only urbanized area in the area of interest (not all land), and the numerator in the calculation is impermeable area. We report this indicator as a time series for the years 1990, 1995, 2000, 2005, 2010, and 2015. These are the years for which we have both the Tsinghua impervious-area data and the urban-extent data.

LIMITATIONS

These calculations are based entirely on remotely sensed data, which we did not assess against local ground truth data. The two datasets compared are in different resolutions and assess different years, which presents difficulties for precise comparison.

FLD-5: vegetation cover in built areas

DEFINITION

The percentage of built land cover without vegetation.

IMPORTANCE

Vegetation cover provides many benefits in urban areas. For flood mitigation, greater vegetation cover can increase water infiltration into the ground, reducing water stagnation and runoff on the surface. In turn, an absence of vegetation cover can increase the prevalence of localized flooding.

METHODS

As with ACC-7, we identified areas as vegetation covered if their fractional vegetation (Fr) was equal to or greater than 0.6. Zhang et al. (2023) report that urban heat islands are best mitigated where fractional vegetation exceeds 0.6. We then compared these areas to built-up areas in the city as defined by the built-up class from ESA WorldCover for the same year of interest. For each city and city district, we calculated at a 10 m

scale the number of built-up pixels and the number of vegetated built-up pixels. Then we calculated the percentage of built-up pixels that were vegetated.

We have implemented this indicator for 2020 and 2021. As future years of WorldCover data become available, it will be practical to report this indicator in the form of a percentage change from earlier years.

LIMITATIONS

These calculations are based fully on remotely sensed data, which we did not assess against local ground truth data. We used an annual mosaic to assess the greenest point in the year for each individual pixel; as a result, this assessment does not measure the state of vegetation at any one point in time but rather the maximum state of vegetation during the year. This estimates for each pixel a combination of the amount of vegetation and state of greenness at peak greenness. In most pixels, the amount of vegetation does not change (except for leaves), but using the peak greenness allows us to estimate how much vegetation exists. Temporal and seasonal changes in vegetation (e.g., vegetation that sheds foliage or goes dormant seasonally) are known to affect the ability of green space to deliver expected benefits such as stormwater mitigation. The benefits in areas with seasonal change will not be as high as those in evergreen ecosystems or where there is no seasonal change (Wilson et al. 2022).

FLD-6: vegetation cover in riparian zones

DEFINITION

The percentage of riparian areas without vegetation or water cover.

IMPORTANCE

Riparian areas—the spatial interface between land and water, particularly rivers and streams—can serve as natural infrastructure for flood control. Whereas in many urban areas these areas have been developed, paved over, or channelized, the presence of vegetation cover in the riparian zone is a primary factor in determining its flood mitigation effectiveness; vegetation can slow down water flow as well as increase its absorption into land and its transpiration into the air (Croke et al. 2017). Riparian areas are also critical habitats that support biodiversity.

METHODS

For this indicator, we used data on elevation and drainage channels from the Global 30m Height Above the Nearest Drainage dataset and on the location of water bodies from the Joint Research Centre (JRC) Global Surface Water dataset (Pekel et al. 2016)[18] to estimate the location of lakes, rivers, and streams. To identify riparian zones, we buffered these waterways by 144 m—the estimated size of riparian areas often needed to preserve significant bird diversity (Lind et al. 2019)—and excluded the area of the water channel itself. To assess vegetation and water cover, we used the NDVI-derived fractional vegetation (*F*r) as calculated in ACC-7, and the Normalized Difference Water Index using the McFeeters (1996) Minimum Threshold method as described in LND-4, with minimum thresholds of 0.6 and 0.5, respectively (Zhang et al. 2023; McFeeters 1996). For the buffered riparian areas in each city or subcity unit, we calculated at a 30 m scale the count of all riparian-area pixels and the count of riparian-area pixels with vegetation or water cover. Then we calculated the percentage of riparian-area pixels without vegetation or water cover.

This indicator is reported as a time series of annual values beginning with the year 2017.

LIMITATIONS

These calculations are based entirely on remotely sensed data, which we did not assess against local ground truth data. In particular, the general definition of *riparian zone* used may not match the situation on the ground as characterized with additional local data, such as in the case of extreme topography adjacent to drainage channels.

FLD-7: steep slopes without vegetation

DEFINITION

The percentage of steep hillside slopes without vegetation cover.

IMPORTANCE

Steep slopes are vulnerable to landslides, especially during incidents of extreme precipitation or flooding, where soil can become saturated with or washed away by water. Vegetation is critical for stabilizing slopes; roots hold soil in place, and plants absorb water from the soil. Steep slopes without vegetation cover are particularly vulnerable to erosion, which can undermine the entire slope's stability and lead to landslides.

METHODS

To estimate slopes on land, we applied the Google Earth Engine slope algorithm (GEE 2022) to the global NASA NASADEM 30 m digital elevation model (NASA JPL 2020). The slope layer was then masked to include high slope areas of only 10 degrees or greater—the threshold at which landslide susceptibility starts to grow quickly (Stanley and Kirschbaum 2017). We estimated vegetation cover using fractional vegetation (*F*r) as calculated for ACC-7. For the high slope areas in each city or subcity unit, we calculated at a 30 m scale the count of all high-slope pixels

and the count of high-slope pixels with any 10 m Sentinel-2 subpixels not meeting a *Fr* threshold of 0.6. Then we used these values to calculate the percentage of high-slope pixels without vegetation cover.

This indicator is reported as a time series of annual values beginning with the year 2017.

LIMITATIONS

These calculations are based entirely on remotely sensed data, which we did not assess against local ground truth data. The digital elevation model is based on data collected in 2000, which may be outdated if significant changes have occurred in local slopes. Additionally, its relatively low resolution (30 horizontal m) may not capture important smaller-slope details.

This indicator combines data from the NASADEM elevation dataset and data from the Sentinel-2 satellite mission for fractional vegetation. Geometric misalignment among remote-sensing products can cause small spatial inaccuracies in the resulting derived data.

Climate change mitigation (GHG)

Cities are responsible for most human-produced greenhouse gas emissions, but cities are also efficient at using resources and can reduce emissions through innovations to mitigate climate change. These indicators consider how cities contribute to climate change, including by measuring the contribution of economic sectors, gases, and activities. For these indicators, higher values are associated with higher greenhouse gas emissions.

GHG-1: greenhouse gas emissions

DEFINITION

Annual cumulative greenhouse gas emissions (measured in carbon dioxide equivalent, or CO_2e) from a city area, disaggregated by pollutant and sector.

IMPORTANCE

Human activity contributes to air pollution and climate change through greenhouse gas emissions from fuel combustion, industrial processes, and agriculture. This indicator can help decision-makers and stakeholders identify the most important pollutants emitted locally, the activities responsible for the emissions, and, with multiple years of data, emissions trends.

METHODS

This indicator is based on the CAMS Global Anthropogenic Emissions dataset (Granier et al. 2019). The dataset provides estimates of emissions from 12 sectors of human activity, on a 0.1-degree (approximately 11 km) spatial resolution. The estimates are based on simulations and historical data. The included sectors are agriculture (livestock); agriculture (soils); agriculture (waste burning); power generation; fugitive emissions; industry;

Table 3 | **Global warming potential of each pollutant species**

POLLUTANT SPECIES	INCLUDED AS GHG	GWP (20-YEAR CO_2 EQUIVALENT)	GWP SOURCE
Ammonia (NH_3)	No	N/A	N/A
Black carbon (BC)	Yes	460	Global values reported in IPCC AR5, Table 8.A.6
Carbon dioxide (CO_2)	Yes	1	Definition of GWP
Carbon monoxide (CO)	Yes	7.65	Midpoints of global values reported in IPCC AR5, Table 8.A.4
Methane (CH_4)	Yes	84	Global values reported in IPCC AR5, Table 8.A.1
Nitrogen oxides (NO_x)	Yes	19	Global values reported in IPCC AR5, Table 8.A.3
Non-methane volatile organic compounds (NMVOCs)	Yes	14	Global values reported in IPCC AR5, Table 8.A.5
Organic carbon (OC)	Yes	–240	Global values reported in IPCC AR5, Table 8.A.6
Sulfur dioxide (SO_2)	No	N/A	N/A

Note: Abbreviations: GHG = greenhouse gas; GWP = global warming potential; CO_2 = carbon dioxide; IPCC = United Nations Intergovernmental Panel on Climate Change; AR5 = Fifth Assessment Report of the IPCC; N/A =not applicable.

Source: Myhre et al. 2013.

combustion in residential, commercial, and other settings; ships; solvents; solid waste and wastewater; off-road transportation; and on-road transportation.

We used Google Earth Engine to calculate the emissions from within our areas of interest (city administrative boundaries). We extracted annual, sector-disaggregated emissions in tonnes/year for each year, for each pollutant species. In our implementation, we also provide annual summaries of total emissions. Because of the coarse resolution of this dataset, we report values for the geographic area of only the full city and not for each subcity area. To have a shared unit of measurement for all species of emissions, we converted tonnes to CO_2e based on the 20-year global warming potentials (EPA n.d.) as listed in Table 3. To produce a summary number for the final indicator, we shared the cumulative CO_2e for each year beginning in 2000 as a time series. Future updates will depend on continued updates to the CAMS data.

LIMITATIONS

The emissions data used for this indicator account for only direct emissions from activities within the boundaries of the city (Scope 1 emissions). These data do not account for emissions associated with electricity that is used in the city but generated elsewhere (Scope 2) or emissions produced elsewhere associated with products or services consumed in the city (Scope 3). The CAMS dataset is modeled data based on an ensemble of multiple emissions models and is subject to the limitation of those models. The methods used to develop the CAMS emissions dataset are described in Granier et al. (2019).

GHG-2: impact of trees on greenhouse gases

DEFINITION

Annual greenhouse gas net flux from trees per hectare (ha) of city area, measured in megagrams (Mg) of CO_2e/ha.

IMPORTANCE

Trees are critical contributors to a balanced climate system. Whereas healthy, growing trees remove carbon from the atmosphere and sequester it, trees that are cut or die emit carbon (Gibbs et al. 2022). Cities can work to keep forests and trees healthy and invest in expanding tree cover to increase carbon removal and reduce trees' contribution to climate change (Pool et al. 2022; Wilson et al. 2022).

METHODS

We calculated this indicator using the Net Carbon Flux from Forests dataset (Version 1.2.2) per Harris et al. (2021), as accessed on Google Earth Engine.[19] This 30 m resolution data layer provides an estimate of net carbon flux from trees (gross emissions minus gross removals) from 2001 through 2021 inclusive in units of Mg CO_2e/ha. To calculate the mean annual carbon flux for each area of interest, we first unmasked the dataset; then pixels where the dataset showed no carbon flux were given a value of 0 and were included in subsequent calculations. Next, we calculated the mean for the area to estimate the average carbon net flux per hectare from the area of interest during each year. As we were interested in measuring city and area characteristics based on their full geographies, not just forest areas, we normalized net flux using total area as the denominator.

We report this indicator as a time series of annual values. Negative numbers represent net greenhouse gas removals, and positive values indicate net emissions.

LIMITATIONS

The carbon flux model used for the calculations was designed for forests and is based on tree cover as detected by Landsat, which means it does not pick up or measure carbon flux from sparse tree cover. At a 30 m resolution, Landsat and products developed from it do not pick up isolated trees. Additionally, the model is limited to pixels with tree canopy density greater than 30 percent and trees of at least 5 m in height, so low-density and short-tree cover are not included. Other limitations of the net flux data are described in Harris et al. (2021).

This indicator does not measure the impacts of indirect land-use change or the greenhouse gas implications of land-use decisions outside its borders. For instance, if a city chooses to avoid developing a green area within its borders, this may lead to exporting the development to nearby suburban areas, possibly resulting in the loss of a greater number of trees and increased transportation demand, both of which could increase net carbon emissions. When making decisions related to land use, cities should consider both the direct and indirect impacts of those decisions.

Heat (HEA)

Due to the urban heat island effect, cities and their residents are exposed to greater heat hazard than equivalent rural areas. Climate change is expected to further exacerbate this risk to cities. These indicators measure local heat hazard and the presence of heat-mitigating infrastructure. For these indicators, higher values are associated with greater hazard, exposure, or vulnerability.

HEA-1: expected annual number of heat waves

DEFINITION

The expected number of heat waves annually over a 10-year period.

IMPORTANCE

Heat waves, or extended, nonoverlapping periods of abnormally high temperatures, are among the deadliest climate phenomena (Nunes 2024; Matthews et al. 2025). Beyond direct health impacts, they can strain economies and energy infrastructure (Burillo et al. 2019; García-León et al. 2021). Understanding the future dynamics of heat waves can inform planning for extreme heat events and assessment of investment needs and opportunities for heat mitigation.

There is no globally accepted definition of *heat wave*. Definitions vary in what durations are considered "extended periods," what temperatures are considered "abnormally high," and even which temperature to consider (e.g., daytime high temperature, nighttime low temperature, 24-hour mean temperature). We adopted a definition that is meant to be generally useful: three or more consecutive days on which the daily maximum temperature exceeds the local 97.5th percentile. The 97.5th percentile is similar to using the 90th percentile, as recommended by Xu et al. (2016), but considers only the warmest one-quarter of the days. As our definition is based on locally calculated extremes, rather than on a single extreme applied globally, this indicator is suited to address changes in cities' climates and the potential for mismatches between future heat hazard and past or existing measures for coping with heat.

METHODS

We defined a heat wave as three or more consecutive days on which the daily maximum temperature exceeded the local 90th percentile of daily maximum temperature, calculated for summertime months (June, July, and August in the northern hemisphere, and December, January, and February in the southern hemisphere) in the years 1980–2014 for the pixel that includes the city centroid. The historical data are from the ERA daily reanalysis dataset (Hersbach et al. 2020).

Similar to FLD-2, this indicator is the expected value of the number of heat waves, based on a probability model parameterized using model outputs from the NEX-GDDP-CMIP6 ensemble of downscaled global climate simulations (NASA 2023). We were able to estimate expected values over 10-year future periods, for any decade ending in or before 2100, with simulations using either the SSP2-4.5 middle-of-the-road or the SSP5-8.5 high-emissions scenarios (Riahi et al. 2017). Details on the probability modeling are in Wong and Switzer (2023).

The spatial resolution of the NEX-GDDP-CMIP6 climate simulations is 0.25 degrees, or approximately 25 km. This resolution is too coarse to inform most subcity decision-making, so we report this indicator as three numbers for the decade of interest—the estimates from the three NEX-GDDP-CMIP6 models whose historical temperature predictions are closest to the ERA5 historical data—estimated at the centroid of the city or district. We currently report this indicator for three decades—2020–29, 2040–49, and 2060–69—using SSP2-4.5.

LIMITATIONS

The limitations of climate models and our method of estimating expected values described for FLD-2 apply here.

Many of the climate models do not consider the presence of buildings or pavement, and any such treatment in a global climate model is necessarily highly simplified. Our method does include a calibration step, whereby the NEX-GDDP-CMIP6 outputs are corrected using the historical ERA5 reanalysis data, but even so they are likely to underestimate temperatures that are elevated by the urban heat island effect. The indicator therefore probably underestimates heat wave frequencies, especially in the most built-up parts of cities.

Our heat wave definition might not be the most relevant for some planning applications. For example, heat waves defined by nighttime temperature might be more important for understanding health impacts for particular age and sex groups (Majeed and Floras 2022).

A more detailed discussion of our heat wave indicators is in Wong and Mackres (2024).

HEA-2: expected highest annual temperature

DEFINITION

The expected highest temperature in one year over a 10-year period.

IMPORTANCE

Whereas the heat wave indicator HEA-1 is intended to address threats to public health, this indicator is designed to address potential risk to infrastructure. Outdoor infrastructure like bridges, rails, and power transformers can all be damaged by extreme temperatures (Underwood et al. 2017; Burillo et al. 2019). Understanding future temperature extremes can help infrastructure engineers with long-term capital planning and risk management.

METHODS

As with HEA-1, we calculated this indicator from a probability model parameterized with outputs from NEX-GDDP-CMIP6 climate models (Wong and Switzer 2023).

We currently report this indicator for three decades—2020–29, 2040–49, and 2060–69—using SSP2-4.5.

LIMITATIONS

This indicator is based on estimates of probabilities as modeled by climate simulations. There are unavoidable errors—including climate stochasticity, scientific uncertainty regarding Earth system processes, and uncertainty in future greenhouse gas emissions trends—from numerous sources. Notably, we used the expected value of a random variable to capture information about a probability distribution in a single number. It should not be interpreted as a prediction.

HEA-3: land surface temperature

DEFINITION

The percentage of built land with a high land surface temperature (LST), defined as greater than or equal to 3 degrees Celsius (°C) above the mean for built land, during the hot season.

IMPORTANCE

LST is correlated with near-surface air temperature, which is one important dimension of how people experience heat. This metric can identify areas of the city exposed to above-average heat. Such areas may be good candidates for heat mitigation measures such as increased tree or vegetation cover or solar reflective surfaces.

METHODS

For this indicator, we used LST for each pixel in the area of interest calculated using the methods from Ermida et al. (2020) and Landsat imagery, at a 30 m resolution, as retrieved from Google Earth Engine. We defined the local hot season as the 90-day calendar interval centered on the date of the hottest day in the years 2013–22 as determined from the ERA5 daily aggregates (Hersbach et al. 2020). We calculated LST from a mosaic of cloud-masked Landsat images from this hot season, over the same years. This collection of LST images was then masked for the built-up class in the ESA WorldCover data. We then retrieved the mean LST value for each unmasked pixel. Finally, areas that were 3°C or more above the area average were masked to calculate the percentage of built area with high LST.

LIMITATIONS

LST is not a direct measure of how people in cities experience heat, which is more closely related to near-surface air temperature and heat indices. Additionally, for this indicator, we used measurements from the times of day at which Landsat retrieves images, usually within a few hours of midday locally. As a result, this indicator does not measure heat in the evening or at night, which is important for understanding local heat impacts. Finally, because we used an image mosaic to remove cloud cover and provide an average for the hot season in the location, the indicator does not reflect any one year, day, or heat event.

HEA-4: surface reflectivity

DEFINITION

The percentage of built land with low surface reflectivity, defined as below 0.2 albedo.

IMPORTANCE

This indicator can identify areas of the city with a high share of surfaces that retain excess heat. Surfaces with low solar reflectivity (albedo) absorb heat and transfer it to the immediate surroundings. Areas with a high share of low albedo surfaces may be candidates for installing measures—such as trees or solar reflective roofs and pavements—that will reduce the heat retained on surfaces or otherwise cool the immediate area.

METHODS

For this indicator, we used pixel-wise albedo values derived from Sentinel-2, at a 10 m resolution, as retrieved from Google Earth Engine using the algorithms defined by Bonafoni and Sekertekin (2020). We calculated annual mean albedo from cloud-free pixels from 2021. We derived values for built land cover areas only using the built-up class from the 10 m resolution ESA WorldCover dataset as a mask. Finally, pixels with albedo values below 0.2—a common threshold used for defining moderately reflective surfaces (Energy Star n.d.)—were masked to calculate the percentage of built area with low surface reflectivity.

LIMITATIONS

These calculations are based fully on remotely sensed data, which are subject to atmospheric interference and other challenges in data collection and which we did not assess against local ground truth data. For this indicator, we used an image mosaic to remove cloud cover and provide an annual average; thus, the indicator does not reflect the situation at any one point in time.

HEA-5: built land without tree cover

DEFINITION

The percentage of built land without tree cover.

IMPORTANCE

This indicator can identify city areas without significant tree cover and therefore those lacking in shade and evapotranspiration that can reduce local heat. Tree cover in built areas varies significantly across cities. Tree cover can provide a cooling effect, documented to be in the range of 3°C (Wang et al. 2018), in urban areas. Areas without tree cover are often exposed to a higher extreme heat hazard. Areas with low tree cover may be candidates for implementing heat mitigation measures—such as trees, other vegetation, or solar reflective roofs and pavements—that will reduce the heat retained locally or otherwise cool the immediate area.

METHODS

As in ACC-2, we used the Meta-WRI Global Canopy Height dataset (Tolan et al. 2024) and defined tree cover as locations with tree height of at least 3 m. We used the built-up class for 2020 from ESA WorldCover to mask the tree cover layer. Because the canopy-height dataset has a spatial resolution of 1 m, we reduced the spatial resolution of the classified dataset to 100 m to match WorldCover. Each pixel of the reduced-resolution data represents the fraction of its component 1 m pixels that were classified as having canopy cover. The percentage of built land with tree cover is the average of the unmasked pixel values, times 100. We then inverted this value for percent tree cover to derive a value for the percentage of built-up land without tree cover.

LIMITATIONS

The limitations associated with the Meta-WRI Global Canopy Height dataset as described in ACC-2 also apply to this indicator.

Land protection and restoration (LND)

Cities play an important role in protecting and restoring natural lands. These lands provide ecosystem services to cities, habitat to wildlife, and other benefits. These indicators classify and measure the characteristics of land within the city and changes over time. For these indicators, higher values are associated with greater protection of natural, nature-like, or otherwise undeveloped land uses within city boundaries.

LND-1: permeable areas

DEFINITION

The percentage of land area that has a permeable (pervious) surface.

IMPORTANCE

Impervious areas are areas in which pavement or other surfaces prevent water from infiltrating the soil. As climate change in many places will change precipitation regimes, many cities with large areas of impervious surfaces will experience high peaks in water runoff, resulting stormwater flooding, and damage to infrastructure and natural areas. This type of flooding also lowers the quality of receiving waters fed by surface water runoff, impacting water quality for the biodiversity of aquatic and marine systems downstream.

METHODS

We calculated this indicator by measuring the proportion of all permeable areas to the total terrestrial area of the city using the following equation:

$$100\% \times \frac{\text{total permeable area}}{\text{total area of city}}$$

Permeable areas were taken from the Global Artificial Impervious Area impervious surface dataset (Gong et al. 2020), which classifies land at a 30 m spatial resolution as permeable or impermeable to water based on vegetation dynamics, water content, and reflectance. Water bodies and undeveloped land were assumed to be permeable. This indicator is similar to FLD-4, with two distinctions: It considers all land in the area of interest (not just land within the urban extent), and the numerator in the calculation is permeable area (not impermeable area). We report these data for years of interest 1985–2018. Values for a series of years can be reported as a time series.

LIMITATIONS

These calculations are based entirely on remotely sensed data, which we did not assess against local ground truth data. Other variables that factor into permeability that are not detectable with remote sensing, such as soil type and use of permeable paving surfaces, are not considered in this analysis.

This dataset has not been updated since 2018.

LND-2: tree cover

DEFINITION

The percentage of land area that has tree cover.

IMPORTANCE

Trees provide numerous services to cities. They provide cooling, improve air quality, store carbon, reduce noise pollution, and regulate the water cycle. Trees also provide habitat for birds, insects, and mammals, and generally improve local ecosystem health (Wilson et al. 2022).

METHODS

For this indicator, we used the 1 m Meta-WRI Global Canopy Height dataset (Tolan et al. 2024). For a land pixel to count as being tree-covered, canopy height must have equaled or exceeded 3 m. We used the following formula:

$$100\% \times \frac{\text{area with tree cover}}{\text{total area of city}}$$

This indicator differs from indicator HEA-5 in two ways: It is calculated over the entire area of interest (not just built-up areas within it), and it counts the areas with tree cover (rather than those without).

LIMITATIONS

The limitations associated with data from the Meta-WRI Global Canopy Height dataset, as described in ACC-2, also apply to this indicator.

LND-3: percent of area covered with high vegetation cover

DEFINITION

Percentage of area with fractional vegetation exceeding 0.6.

IMPORTANCE

Vegetation provides many ecosystem services to cities, including stormwater management, temperature moderation, and habitat for urban wildlife. This indicator supports planning and monitoring in vegetation management. It also supports the IUCN Urban Nature Indexes Indicator 3.4 (IUCN 2023).

METHODS

We calculated fractional vegetation (*F*r) for every 10 m pixel within the city boundary, following the method described in ACC-7. We considered a pixel area to be covered by vegetation if its $F_r \geq 0.6$. Zhang et al. (2023) report that urban heat islands are best mitigated where fractional vegetation exceeds 0.6.

We calculated the percent covered using the following equation:

$$100\% \times \frac{\text{number of pixels with } F_r \geq 0.6}{\text{total number of pixels within city boundary}}$$

The indicator is reported as a time series of annual values beginning with 2017.

LIMITATIONS

The limitations of fractional vegetation described in ACC-7 apply to this indicator. Note that this indicator does not address vegetation type. Local knowledge is necessary to consider differences in species, growth habit, and seasonality that are relevant to particular vegetation-management applications.

This indicator reports the percentage of pixels whose fractional vegetation values exceeded a threshold. Some users might confuse this with the fractional vegetation value of the entire area of interest, and in fact might prefer such an indicator. In the future we might change this indicator to the fractional vegetation of an entire area of interest, or add it as a new indicator, if it is useful for our target audience.

LND-4: percentage of area covered by water

DEFINITION

Percentage of area covered by water.

IMPORTANCE

Water cover provides many ecosystem services to cities, including groundwater recharge, flood management, temperature moderation, and support for wildlife.

METHODS

We used 10 m Sentinel-2 data, as accessed on Google Earth Engine, and cloud masked (ESA 2015a) to calculate the Normalized Difference Water Index (NDWI) as described by McFeeters (1996). We created annual bluest-pixel mosaics for each year following the Minimum Threshold method, which Sekertekin (2021) found to have the greatest accuracy among 15 tested thresholding methods. Based on this method, we repeatedly smoothed the histogram of the NDWI values to produce a histogram with two local maxima, and we took as the threshold

($NDWI_{thresh}$) that separates non-water from water pixels the NDWI value between the two maxima with the lowest histogram density. We calculated the percent covered by water using the following equation:

$$100\% \times \frac{\text{number of pixels where } NDWI \geq NDWI_{thresh}}{\text{total number of pixels within city boundary}}$$

We report this indicator as a time series for the years 2017–present.

LIMITATIONS

This indicator is based on interpretation of satellite data, and it is likely to be less accurate than methods based on locally acquired data from land surveys and water-monitoring programs. For example, it does not distinguish between water bodies of different depth, water quality, or other hydrological characteristics.

LND-5: habitat area restored

DEFINITION

The area of habitat land restored between two years of interest as a percentage of habitat land in the base year.

IMPORTANCE

Cities can directly improve biodiversity by converting poor habitat or nonhabitat land to good habitat. Good habitat generally includes multispecies vegetation and enough structural complexity to provide shade and cover from predators. The IUCN Urban Nature Indexes Indicator 3.2 and Singapore Index Indicator 7 call on cities to either estimate the area of land restored to "good ecological functioning" or enumerate the types of habitat restored. This indicator supports the area-of-land-restored method.

METHODS

We were unable to discern habitat quality using global data, but we could provide data on changes in land classification from nonhabitat classes to habitat classes. We used the Landsat Analysis Ready Data (Potapov et al. 2022) from the Global Land Analysis and Discovery research group at the University of Maryland.[20] In our implementation, we defined habitat as aquatic or noncropland vegetated classes, and we compared classifications from 2000 as the base year, or year 1, and 2020 as year 2. We defined new habitat as pixels that were classified as nonhabitat (urban, cropland, or bare) in year 1 but as habitat in year 2. We calculated this indicator using the following equation:

$$100\% \times \frac{\text{area of habitat in year 2 that was nonhabitat in year 1}}{\text{area of nonhabitat in year 1}}$$

LIMITATIONS

This method differs somewhat from what is described in the Singapore Index Indicator 7. Our denominator is nonhabitat rather than degraded habitat. Degraded habitat was habitat in the recent past, but nonhabitat includes degraded habitat and land that has long been converted to other uses. Our estimate therefore probably underestimates restoration as measured by this indicator.

The Landsat Analysis Ready Data dataset is currently available only for 2000 and 2020. We will add comparisons for additional pairs of years if more data become available.

LND-6: habitat types restored

DEFINITION

The number of habitat types restored between two years of interest as a percentage of all habitat types in the area.

IMPORTANCE

Cities can directly improve biodiversity by converting poor habitat or nonhabitat land to good habitat. Good habitat generally includes multispecies vegetation and enough structural complexity to provide shade and cover. Indicator 7 in the Singapore Index calls on cities to either estimate the area of land restored to "good ecological functioning" or enumerate the types of habitat restored. This indicator supports the habitat-type enumeration method.

METHODS

We calculated this indicator using the following formula:

$$100\% \times \frac{\text{number of habitat types restored}}{\text{number of habitat types in city in baseline year}}$$

The Landsat Analysis Ready Data discern six land cover classes that we included as types of habitat: short vegetation, forest, tall forest (taller than 20 m), wetland with short vegetation, wetland forest, and open water. (We treated the classes for bare ground, snow or ice, cropland, and built-up area as nonhabitat.) We calculated our indicator by identifying areas of new habitat, where habitat existed in year 2 but not in year 1 or the base year; counting the number of habitat types (i.e., aquatic and vegetated land cover classes) in these areas of new habitat; and comparing this number to the total number of habitat types in the city in year 2. For example, consider a city that had four types

of habitat in 2020. We took 2020 as year 2 and looked for all habitat areas in 2020 that were nonhabitat in the baseline year 2000 and considered these to be new habitat areas. If there were two habitat types in the new habitat areas, we calculated the indicator as follows:

$$100\% \times \frac{\text{2 habitat types in new habitat}}{\text{4 habitat types in city in 2020}} = 50\%$$

LIMITATIONS

This indicator describes restoration as a fraction of the existing diversity of habitat types, not as the absolute diversity of restored habitat. It does not distinguish between a city that restores many types of habitat and a city that simply has few habitat types. For example, in a city with six habitat types, restoration of six types of habitat will result in an indicator value of 100 percent. The indicator is also 100 percent if a city with just one habitat type restores just one habitat type. By scaling restored diversity by overall diversity, this indicator focuses narrowly on cities' efforts to restore native diversity and not on the diversity itself.

Our method also differs from that of the Singapore Index: We used new habitat instead of habitat that had been improved from degraded to good ecological function. Cities that have access to local data specifically detailing the extent and status of habitat restoration projects would probably benefit from calculating the Singapore Index Indicator 7 using those data.

LND-7: protected areas

DEFINITION

The percentage of land area that is designated as protected area.

IMPORTANCE

Protected or secured natural areas indicate a government's legally formalized commitment to conserve biodiversity. Protected areas are lands (or waters) with legal restrictions on development or use and sometimes physical barriers to entry. Protected areas inside and near cities, including outside their jurisdictional boundaries, can provide multiple benefits to people living in cities in the form of human health and well-being and water security (Wilson et al. 2022). Importantly, they serve as havens for biodiversity and can be used to create ecological connectivity and restore previously lost biodiversity in the cityscape. This indicator supports the IUCN Urban Nature Indexes Indicator 3.1.

METHODS

We calculated this indicator using the following formula:

$$100\% \times \frac{\text{area of protected or secured natural areas within city}}{\text{total area of city}}$$

Our data on protected areas come from the World Database on Protected Areas (WDPA), which is a collection of data on protected areas contributed by national governments (UNEP-WCMC and IUCN n.d.).

LIMITATIONS

- This indicator measures only protected areas within city boundaries, excluding nearby protected areas.
- The WDPA is based on information contributed by national governments. It might exclude areas whose protections do not fit criteria set by these governments.
- Intensive, biodiversity-harming activities can occur within formally protected areas. We did not assess specific legal protections; nor did we assess enforcement of protections.
- Because of the nature of the source WDPA data, we were unable to report this indicator as a time series of annual values.

LND-8: protection of Key Biodiversity Areas

DEFINITION

The percentage of Key Biodiversity Area (KBA) land that is designated as protected area.

IMPORTANCE

KBAs are areas that have been identified by the KBA Partnership as being important to global biodiversity, generally because they include either a globally important type of habitat or because they include habitat for a globally important species (BirdLife International 2022). Criteria for inclusion include the presence of threatened biodiversity, the presence of geographically restricted biodiversity, ecological integrity, critical biological processes, and irreplaceability. Cities can threaten or contribute to the global persistence of biodiversity through their development choices. Limiting development within KBAs or formally protecting land within KBAs can protect biodiversity in these areas.

In addition to the map of local KBAs, we provide two indicators related to these areas (LND-7 and LND-8). Neither indicator corresponds directly to an indicator in the Singapore Index.

METHODS

KBAs can often benefit from formal protection (KBA Partnership 2017). In this indicator, we provide information on how much of a city's KBA is currently under formal protection. This is the formula:

$$100\% \times \frac{\text{area of KBA within city under formal protection}}{\text{total area of KBA within city}}$$

KBA data are provided by BirdLife International (2022) for the KBA Partnership, and data on protected areas come from the WDPA (UNEP-WCMC and IUCN n.d.).

LIMITATIONS

This indicator shares the limitations of LND-7 arising from limitations in the WDPA. Both the WDPA and the KBA data are periodically updated. Those who use values of this indicator calculated by WRI or others should note whether they were based on the most recent versions of the input data.

The terms of use provided by the KBA Partnership do not allow us to share the source KBA data, but all data can be requested from BirdLife International. Similarly, the United Nations Environment Programme World Conservation Monitoring Centre and the International Union for Conservation of Nature do not allow us to share the source data on protected areas, but all data are available on the WDPA website (https://www.protectedplanet.net).

LND-9: undeveloped Key Biodiversity Areas

DEFINITION

The percentage of KBA land that is not built up.

IMPORTANCE

Land expansion from cities and other settlements poses a major threat to biodiversity (McDonald et al. 2018). Habitat quality in built-up areas tends to be lower than in natural areas. Habitat quality in KBAs might therefore be improved by habitat restoration efforts that convert built-up areas to natural ecosystem types.

METHODS

We provide an indicator that describes how much of the KBA within the city is built up. The formula is as follows:

$$100\% \times \left(1 - \frac{\text{built up area in KBA within city}}{\text{total area of KBA within city}}\right)$$

The data on built-up areas are from the 2020 ESA WorldCover. KBA data are provided by BirdLife International (2022) for the KBA Partnership.

LIMITATIONS

The KBA data are periodically updated. Those who use values of this indicator calculated by WRI or others should note whether they were based on the most recent versions of the input data.

The terms of use provided by the KBA Partnership do not allow us to share the source data, but all data can be requested on its website (https://www.keybiodiversityareas.org).

General limitations

The indicators developed through these methods can provide numerous insights on variations within and between cities and changes over time. However, there are limitations to the value provided by these indicators, uncertainty regarding the resulting indicator values, and caveats to their meaning and potential applications that should be understood. In addition to the limitations specific to each indicator mentioned, there are also a few general methodological constraints. We have addressed these concerns to the extent practical in how specific indicators are defined and presented, but these issues remain important for users of the indicators.

- **Boundaries and aggregations.** These methods primarily focus on providing a summary value of each area of interest for each indicator. Doing so helps simplify a large number of data, but it can also obscure nuance and important information. First, the areas of interest need to be meaningful. We used administrative areas because they are important boundaries of authority for decision-makers and are often used to aggregate other information. But different boundaries result in different indicator values. Other boundaries may be more relevant to a different set of stakeholders in the same city. Boundaries can change over time, making comparisons difficult. And for some topics, other kinds of boundaries may be more appropriate to generate meaningful insights (e.g., watershed boundaries for hydrology). Second, how boundaries are drawn and the characteristics of the areas within the boundaries can profoundly affect the results of data aggregations for the area of interest. As an example, if a park is equally split between two city wards that have similar vegetation coverage, the boundaries could obscure the significant vegetation differences within their respective residential areas due to averaging. If the park is classified as a separate area of interest, a vegetation cover indicator would more accurately

characterize the differences between the two remaining residential areas. Third, the size of the areas of interest in comparison to the scale of the datasets used to calculate indicators can produce results that range from insightful to nearly meaningless. For example, assume a city has equally sized square districts of 1 km in each direction. A raster dataset that is at a smaller scale would give useful information about the area within the district (but if it is much smaller in scale, such as 10 m, it may give too much information for an aggregate indicator to fully summarize, as we discuss further below). However, if the dataset is of a larger scale, say 10 km, aggregations at the smaller district scale result in the same value for many districts, which likely does not reflect the reality on the ground and does not give any meaningful information for comparison among the districts.

- **Data uncertainty and incompleteness.** The data sources used to calculate the indicators themselves have significant limitations. The global-scale datasets from remote sensing or crowdsourcing used for our indicators are limited by what sensors can detect, their minimum mapping unit, and user contributions. They can give the impression of completeness while not being relevant at the scale of the desired analysis or can be missing important contextual details. We document limitations of specific datasets within the methods' description for each indicator. In contrast, local data pose their own problems, including being limited in scope, using local definitions that are often incompatible with data used elsewhere, introducing bias to an analysis, and often being difficult to access. The time required to collect and process local data makes it impossible to use local data for this project, which aims to calculate shared indicators for eventually hundreds of cities around the world. Ultimately, decisions about the most appropriate data for a local challenge need to be made by or with local stakeholders. For this reason, methods with flexible data input sources are critical. Our indicator methods can be adapted by our team or other researchers for use with similar alternative datasets, including from local sources, if a more appropriate one is developed or identified.
- **Comparability between indicators and datasets.** The differences between datasets—such as their scale or date of acquisition—can make it complex to use multiple datasets together. We intend for multiple indicators to be shared with stakeholders; however, indicators within the same thematic areas, and even indicators themselves, may draw on information from various datasets. Within individual indicators, we often use multiple datasets together (e.g., a primary dataset and another dataset to mask the data to focus on land cover types of interest) to develop an indicator statistic. The best datasets for required variables may be available for different years, meaning some changes during that time period are ignored or misrepresented. Or they may be of different scales, meaning that issues of aggregation (as discussed previously) or precision (e.g., more trees being detectable at a 10 m scale than a 30 m scale) can mean that the datasets show different information in the same place.
- **Spatial observational data are not enough.** Our indicators almost exclusively identify the current physical states or changes to them in cities. This information can establish trends; benchmark areas against each other; and help identify opportunities, diagnose problems, and spatially target interventions. However, the indicators alone are likely not sufficient to identify actions and set targets. Domain expertise and local knowledge to identify options and planning processes to determine objectives are required. Importantly, these indicators do not measure or attribute influences on physical changes, such as policies or infrastructure investment, or their effectiveness. To track progress toward physical goals, observational data are essential. To understand which actions are working well and which are falling short, other data and methods are required.
- **Indicators address single dimensions, while urban sustainability is multidimensional.** Most of our indicators were chosen to address issues in a single theme, but cities must contend with many themes at once. Consider an extended example: Some cities might seek to reduce flood risk, improve support for biodiversity, reduce greenhouse gas emissions, and improve residents' access to urban amenities. Indicator FLD-5 addresses flood risk, and preservation of green space in a matrix of built-up land would be one (but not the only!) strategy to improve flood mitigation as reflected in FLD-5. Green space preservation would probably also preserve or promote habitat for some types of wildlife. However, such a strategy might also work against efforts to increase the density of developed land, complicating land-use strategies to improve accessibility of urban amenities and reduce vehicle use. Our indicators are intended to inform city decision-making, but in themselves they do not provide guidance on the difficult, city-specific work of choosing which themes to prioritize and crafting solutions that are best suited to the local environmental, social, and political context.

Further work

These indicator methods and their uses can be further refined and enhanced. Options identified so far include the following:

- Offer guidance on developing new or revised indicators emphasizing designs that are fit for purpose for dataset comparison and selection.
- Develop additional indicators or adapt existing indicator methods into our calculation framework to allow for similar standard measurements on other urban themes relevant to city decision-makers or stakeholders.
- Calculate indicators for additional cities and for other initiatives supporting cities on sustainable development.
- Compare our indicator findings with socioeconomic data to explore relationships among indicators of urban equity and the presence of urban amenities and risk in multiple cities.
- Create a process for vetting and validating new global or local data layers as they become available to potentially integrate with and improve existing indicator methods.
- Compare computed indicators using global data with computations from available local data for validation and provide support to stakeholders for collecting local data as needed.
- Improve integration of user feedback and needs into indicator prioritization, design, and development.
  - Connect more with potential users and stakeholders and define their profiles, statuses, data capacities, and needs.
  - Conduct user needs assessments to better understand how the proposed indicators may help our stakeholders in their decision-making processes and what additional indicators—or modifications to existing indicators—may be useful for users.
  - Map our indicators with potential city-level actions and how the proposed metrics may drive them.
  - Create focus groups or case studies of cities sharing feedback on the value and uses of the data and indicators.

Appendix A. OpenStreetMap key-value pairs

Table A-1 | **Search parameters used in OpenStreetMap queries**

	COMMERCE	EDUCATION	HEALTH CARE AND SOCIAL SERVICES	AGRICULTURE	GOVERNMENT	INDUSTRY	TRANSPORTATION AND LOGISTICS
aeroway: terminal							X
amenity: animal_boarding	X						
amenity: animal_breeding				X			
amenity: animal_shelter	X						
amenity: bank	X						
amenity: biergarten	X						
amenity: bus_station							X
amenity: cafe	X						
amenity: casino	X						
amenity: childcare	X						
amenity: college		X					
amenity: courthouse					X		
amenity: dentist			X				
amenity: doctors			X				
amenity: fast_food	X						
amenity: ferry_terminal							X
amenity: fire_station					X		
amenity: food_court	X						
amenity: hospital			X				
amenity: kindergarten		X					
amenity: library					X		
amenity: mortuary	X						
amenity: music_school		X					
amenity: nightclub	X						
amenity: nursing_home			X				
amenity: pharmacy			X				
amenity: police					X		
amenity: post_office					X		
amenity: prep_school		X					
amenity: research_institute		X					
amenity: restaurant	X						

	COMMERCE	EDUCATION	HEALTH CARE AND SOCIAL SERVICES	AGRICULTURE	GOVERNMENT	INDUSTRY	TRANSPORTATION AND LOGISTICS
amenity: school		X					
amenity: social_facility			X				
amenity: studio	X						
amenity: theatre	X						
amenity: townhall					X		
amenity: university		X					
amenity: veterinary	X						
building: bank	X						
building: clinic			X				
building: college		X					
building: commercial	X						
building: factory						X	
building: government					X		
building: government_office					X		
building: hospital			X				
building: industrial						X	
building: manufacture						X	
building: office							
building: poultry_house				X			
building: pub	X						
building: restaurant	X						
building: retail	X						
building: school		X					
building: shop	X						
building: store	X						
building: supermarket	X						
building: university		X					
building: warehouse							X
cargo: *							X
industrial: *						X	
landuse: animal_keeping				X			
landuse: aquaculture				X			
landuse: commercial	X						

	COMMERCE	EDUCATION	HEALTH CARE AND SOCIAL SERVICES	AGRICULTURE	GOVERNMENT	INDUSTRY	TRANSPORTATION AND LOGISTICS
landuse: education		X					
landuse: farm				X			
landuse: farmyard				X			
landuse: greenhouse_horticulture				X			
landuse: harbour							X
landuse: industrial						X	
landuse: orchard				X			
landuse: paddy				X			
landuse: plant_nursery				X			
landuse: quarry						X	
landuse: retail	X						
landuse: vinyard				X			
railway: station							X
school: *		X					

Note: Key-value pairs relate information (values) to category labels (keys). This table lists the key-value pairs we used to extract data on the locations of urban amenities from OpenStreetMap for indicators ACC-4 through ACC-13. An X indicates that a key-value pair (row) was included in the OpenStreetMap query for a particular amenity class (column). Key-value pairs were combined into a query by OR-relations: We searched for all amenity locations tagged with at least one of the listed key-value pairs. An asterisk (*) indicates that all data tagged with a key, regardless of the associated value, were part of the query.

Source: WRI authors.

Endnotes

1. To learn about the Cities4Forests initiative, visit https://cities4forests.com/.
2. For information about the UrbanShift initiative, see https://www.shiftcities.org/.
3. For more information about the OSM database, see https://www.openstreetmap.org/.
4. NEX-GDDP refers to the National Aeronautics and Space Administration Earth Exchange Global Daily Downscaled Projections. CMIP6 refers to the sixth phase of the Coupled Model Intercomparison Project.
5. The Cities Indicators Framework is an open-source Python package available at https://github.com/wri/cities-cif.
6. To access the WRI Cities Indicators API, visit https://cities-data-api.wri.org/.
7. To access the CityMetrics data dashboard, visit https://www.citymetrics.wri.org/.
8. Key-value pairs describe how data are structured, often in systems that store large volumes of varied data. The key is an identifier, and the value is the information associated with that identifier.
9. To learn more about the Global Anthropogenic Emissions dataset, see https://eccad3.sedoo.fr/metadata/479; for CAMS, see https://atmosphere.copernicus.eu/; and for ECCAD, see https://eccad.aeris-data.fr/.
10. For more information about the CAMS Global Reanalysis EAC4 dataset, visit https://www.ecmwf.int/en/forecasts/dataset/cams-global-reanalysis.
11. To learn more about the V5.GL.02 dataset, see https://sites.wustl.edu/acag/datasets/surface-pm2-5/#V5.GL.02, and for the Atmospheric Composition Analysis Group, see https://sites.wustl.edu/acag/.
12. For more information about the Aqueduct Floods database, visit https://www.wri.org/applications/aqueduct/floods.
13. SSP stands for shared socioeconomic pathway. SSP2-4.5 refers to a middle-of-the-road emissions scenario and SSP5-8.5 to a high-emissions scenario.
14. ERA5 refers to the fifth-generation atmospheric reanalysis dataset produced by the Copernicus Climate Change Service at the European Centre for Medium-Range Weather Forecasts.
15. For additional information about the Global 30m Height Above the Nearest Drainage dataset, see https://gee-community-catalog.org/projects/hand/.
16. For more information about the 2020 ESA WorldCover, visit https://developers.google.com/earth-engine/datasets/catalog/ESA_WorldCover_v100.
17. For more information about the Tsinghua annual maps, see https://developers.google.com/earth-engine/datasets/catalog/Tsinghua_FROM-GLC_GAIA_v10.
18. More information about the JRC Global Surface Water dataset is available at https://developers.google.com/earth-engine/datasets/catalog/JRC_GSW1_3_GlobalSurfaceWater.
19. To access the Net Carbon Flux from Forests dataset, visit https://code.earthengine.google.com/?asset=projects/wri-datalab/gfw-data-lake/net-flux-forest-extent-per-ha-v1-2-2-2001-2021/net-flux-global-forest-extent-per-ha-2001-2021.
20. To learn more about the Global Land Analysis and Discovery research group, visit https://glad.umd.edu/.

References

Alegana, V.A., P.M. Atkinson, C. Pezzulo, A. Sorichetta, D. Weiss, T. Bird, E. Erbach-Schoenberg, et al. 2015. "Fine Resolution Mapping of Population Age-Structures for Health and Development Applications." *Journal of the Royal Society Interface* 12 (105): 20150073.

Amiri, R., Q. Weng, A. Alimohammadi, and S.K. Alavipanah. 2009. "Spatial-Temporal Dynamics of Land Surface Temperature in Relation to Fractional Vegetation Cover and Land Use/Cover in the Tabriz Urban Area, Iran." *Remote Sensing of Environment* 113 (12): 2606–17.

Angel, S., E. Mackres, and B. Guzder-Williams. 2024. "Measuring Change in Urban Land Consumption: A Global Analysis." *Land* 13 (9): 1491.

Avtar, R., R. Aggarwal, A. Kharrazi, P. Kumar, and T.A. Kurniawan. 2019. "Utilizing Geospatial Information to Implement SDGs and Monitor Their Progress." *Environmental Monitoring and Assessment* 192 (December): 35. https://doi.org/10.1007/s10661-019-7996-9.

Bell, C.D., K. Spahr, E. Grubert, J. Stokes-Draut, E. Gallo, J.E. McCray, and T.S. Hogue. 2019. "Decision Making on the Gray-Green Stormwater Infrastructure Continuum." *Journal of Sustainable Water in the Built Environment* 5 (1): 04018016.

BirdLife International. 2022. (Database.) *World Database of Key Biodiversity Areas*. Key Biodiversity Areas Partnership. https://www.keybiodiversityareas.org/.

Bocher, E., G. Petit, J. Bernard, and S. Palominos. 2018. "A Geoprocessing Framework to Compute Urban Indicators: The MApUCE Tools Chain." *Urban Climate* 24 (June): 153–74. https://doi.org/10.1016/j.uclim.2018.01.008.

Boeing, G., C. Higgs, S. Liu, B. Giles-Corti, J.F. Sallis, E. Cerin, M. Lowe, et al. 2022. "Using Open Data and Open-Source Software to Develop Spatial Indicators of Urban Design and Transport Features for Achieving Healthy and Sustainable Cities." *Lancet Global Health* 10 (6): e907–18. https://doi.org/10.1016/S2214-109X(22)00072-9.

Boeing, G. 2024. "Modeling and Analyzing Urban Networks and Amenities with OSMnx." Working Paper. *Geographical Analysis*. https://geoffboeing.com/publications/osmnx-paper/.

Bonafoni, S., and A. Sekertekin. 2020. "Albedo Retrieval from Sentinel-2 by New Narrow-to-Broadband Conversion Coefficients." *IEEE Geoscience and Remote Sensing Letters* 17 (9): 1618–22. https://doi.org/10.1109/LGRS.2020.2967085.

Brown, C.F., S.P. Brumby, B. Guzder-Williams, T. Birch, S.B. Hyde, J. Mazzariello, W. Czerwinski, et al. 2022. "Dynamic World, Near Real-Time Global 10 M Land Use Land Cover Mapping." *Scientific Data* 9 (1): 251.

Buchmueller, T.C., M. Jacobson, and C. Wold. 2006. "How Far to the Hospital? The Effect of Hospital Closures on Access to Care." *Journal of Health Economics* 25 (4): 740–61.

Burillo, D., M.V. Chester, S. Pincetl, and E. Fournier. 2019. "Electricity Infrastructure Vulnerabilities Due to Long-Term Growth and Extreme Heat from Climate Change in Los Angeles County." *Energy Policy* 128: 943–53.

Carlson, T.N., and D.A. Ripley. 1997. "On the Relation between NDVI, Fractional Vegetation Cover, and Leaf Area Index." *Remote Sensing of Environment* 62 (3): 241–52. https://doi.org/10.1016/S0034-4257(97)00104-1.

Chan, L., O. Hillel, P. Werner, N. Holman, I. Coetzee, R. Galt, and T. Elmqvist. 2021. *Handbook on the Singapore Index on Cities' Biodiversity (also Known as the City Biodiversity Index).* CBD Technical Series 98. Montreal: Secretariat of the Convention on Biological Diversity; Singapore: National Parks Board. https://www.cbd.int/doc/publications/cbd-ts-98-en.pdf.

Cochran, F., J. Daniel, L. Jackson, and A. Neale. 2020. "Earth Observation-Based Ecosystem Services Indicators for National and Subnational Reporting of the Sustainable Development Goals." *Remote Sensing of Environment* 244 (July): 111796. https://doi.org/10.1016/j.rse.2020.111796.

Croke, J., C. Thompson, and K. Fryirs. 2017. "Prioritising the Placement of Riparian Vegetation to Reduce Flood Risk and End-of-Catchment Sediment Yields: Important Considerations in Hydrologically-Variable Regions." *Journal of Environmental Management* 190 (April): 9–19. https://doi.org/10.1016/j.jenvman.2016.12.046.

Dai, D. 2010. "Black Residential Segregation, Disparities in Spatial Access to Health Care Facilities, and Late-Stage Breast Cancer Diagnosis in Metropolitan Detroit." *Health & Place* 16 (5): 1038–52.

Deslauriers, M.R., A. Asgary, N. Nazarnia, and J.A.G. Jaeger. 2018. "Implementing the Connectivity of Natural Areas in Cities as an Indicator in the City Biodiversity Index (CBI)." In *Landscape Indicators—Monitoring of Biodiversity and Ecosystem Services at Landscape Level*, edited by U. Walz and R.-U. Syrbe, Special Issue, *Ecological Indicators* 94 (November): 99–113. https://doi.org/10.1016/j.ecolind.2017.02.028.

DiCecco, G.J., V. Barve, M.W. Belitz, B.J. Stucky, R.P Guralnick, and A.H. Hurlburt. 2021. "Observing the Observers: How Participants Contribute Data to iNaturalist and Implications for Biodiversity Science." *BioScience* 71 (11): 1179–88.

Donchyts, G., H. Winsemius, J. Schellekens, T. Erickson, H. Gao, H. Savenije, and N. van de Giesen. 2016. "Global 30m Height above the Nearest Drainage (HAND)." *Geophysical Research Abstracts* 18: EGU2016-17445-3. https://gee-community-catalog.org/projects/hand/.

Energy Star. n.d. "ENERGY STAR Program Requirements for Roof Products: Partner Commitments." Energy Star. https://www.energystar.gov/sites/default/files/specs//Roof%20Products%20V3%20Program%20Requirements_0.pdf. Accessed March 7, 2023.

Engel-Cox, J.A., R.M. Hoff, and A.D.J. Haymet. 2004. "Recommendations on the Use of Satellite Remote-Sensing Data for Urban Air Quality." *Journal of the Air & Waste Management Association* 54 (11): 1360–71. https://doi.org/10.1080/10473289.2004.10471005.

EPA (US Environmental Protection Agency). n.d. "Understanding Global Warming Potentials." https://www.epa.gov/ghgemissions/understanding-global-warming-potentials. Accessed January 12, 2016.

Ermida, S.L., P. Soares, V. Mantas, F.-M. Göttsche, and I.F. Trigo. 2020. "Google Earth Engine Open-Source Code for Land Surface Temperature Estimation from the Landsat Series." *Remote Sensing* 12 (9): 1471. https://doi.org/10.3390/rs12091471.

ESA (European Space Agency). 2015a. "Sentinel-2: Cloud Probability." Earth Engine Data Catalog. https://developers.google.com/earth-engine/datasets/catalog/COPERNICUS_S2_CLOUD_PROBABILITY.

ESA. 2015b. "Sentinel-2 MSI: MultiSpectral Instrument, Level-1C." Earth Engine Data Catalog. https://developers.google.com/earth-engine/datasets/catalog/COPERNICUS_S2.

ESA. 2020a. "ESA WorldCover 10m V100." Earth Engine Data Catalog. https://developers.google.com/earth-engine/datasets/catalog/ESA_WorldCover_v100.

ESA. 2020b. *WorldCover Product User Manual, Version 1.0*. Paris: ESA. https://worldcover2020.esa.int/data/docs/WorldCover_PUM_V1.1.pdf.

Fahrig, L. 2003. "Effects of Habitat Fragmentation on Biodiversity." *Annual Review of Ecology, Evolution, and Systematics* 34: 487–515. https://doi.org/10.1146/annurev.ecolsys.34.011802.132419.

Feng, S., D. Gao, F. Liao, F. Zhou, and X. Wang. 2016. "The Health Effects of Ambient $PM_{2.5}$ and Potential Mechanisms." *Ecotoxicology and Environmental Safety* 128 (June): 67–74. https://doi.org/10.1016/j.ecoenv.2016.01.030.

Fink, C., W. Klumpenhouwer, M. Saraiva, R. Pereira, and H. Tenkanen. 2022. "R5py: Rapid Realistic Routing with R5 in Python." *Zenodo*. doi:10.5281/ZENODO.7060437.

Forman, R.T.T., and M. Godron. 1991. *Landscape Ecology*. Hoboken, NJ: Wiley. https://www.wiley.com/en-us/Landscape+Ecology-p-9780471870371.

Fritz, S., L. See, T. Carlson, M. Haklay, J.L. Oliver, D. Fraisl, R. Mondardini, et al. 2019. "Citizen Science and the United Nations Sustainable Development Goals." *Nature Sustainability* 2 (October): 922–30. https://doi.org/10.1038/s41893-019-0390-3.

García-León, D., A. Casanueva, G. Standardi, A. Burgstall, A.D. Flouris, and L. Nybo. 2021. "Current and Projected Regional Economic Impacts of Heatwaves in Europe." *Nature Communications* 12 (1): 5807.

GBIF (Global Biodiversity Information Facility). 2025. "GBIF Occurrence Download." https://doi.org/10.15468/dl.ef5u6r.

GEE. 2022. "Ee.Terrain.slope." August 1. https://developers.google.com/earth-engine/apidocs/ee-terrain-slope.

Gibbs, D., N. Harris, and J.-R. Pool. 2022. *Global Protocol for Community-Scale Greenhouse Gas Inventories: Supplemental Guidance for Forests and Trees*. Washington, DC: Greenhouse Gas Protocol, World Resources Institute. https://ghgprotocol.org/gpc-supplemental-guidance-forests-and-trees.

Giuliani, G., E. Petri, E. Interwies, V. Vysna, Y. Guigoz, N. Ray, and I. Dickie. 2021. "Modelling Accessibility to Urban Green Areas Using Open Earth Observations Data: A Novel Approach to Support the Urban SDG in Four European Cities." *Remote Sensing* 13 (3): 422. https://doi.org/10.3390/rs13030422.

Gong, P., X. Li, J. Wang, Y. Bai, B. Chen, T. Hu, X. Liu, et al. 2020. "Annual Maps of Global Artificial Impervious Area (GAIA) between 1985 and 2018." *Remote Sensing of Environment* 236 (January): 111510. https://doi.org/10.1016/j.rse.2019.111510.

Gorelick, N., M. Hancher, M. Dixon, S. Ilyushchenko, D. Thau, and R. Moore. 2017. "Google Earth Engine: Planetary-Scale Geospatial Analysis for Everyone." *Remote Sensing of Environment* 202: 18–27.

Grande, A.M., N.W. Chan, P. Gajbhiye, D.J. Perkins, and P.S. Warren. 2022. "Evaluating the Use of Semi-structured Crowdsourced Data to Quantify Inequitable Access to Urban Biodiversity: A Case Study with eBird." *PLOS One* 17 (11): e0277223.

Granier, C., S. Darras, H. Denier van der Gon, J. Doubalova, N. Elguindi, B. Galle, M. Gauss, et al. 2019. "The Copernicus Atmosphere Monitoring Service Global and Regional Emissions (April 2019 Version)." Copernicus Atmosphere Monitoring Service. https://doi.org/10.24380/D0BN-KX16.

Guzder-Williams, B., E. Mackres, S. Angel, A.M. Blei, and P. Lamson-Hall. 2023. "Intra-urban Land Use Maps for a Global Sample of Cities from Sentinel-2 Satellite Imagery and Computer Vision." *Computers, Environment and Urban Systems* 100: 101917.

Harris, N.L., D.A. Gibbs, A. Baccini, R.A. Birdsey, S. de Bruin, M. Farina, L. Fatoyinbo, et al. 2021. "Global Maps of Twenty-First Century Forest Carbon Fluxes." *Nature Climate Change* 11 (3): 234–40. https://doi.org/10.1038/s41558-020-00976-6.

Helmrich, A.M., B.L. Ruddell, K. Bessem, M.V. Chester, N. Chohan, E. Doerry, J. Eppinger, et al. 2021. "Opportunities for Crowdsourcing in Urban Flood Monitoring." *Environmental Modelling & Software* 143 (September): 105124. https://doi.org/10.1016/j.envsoft.2021.105124.

Hersbach, H., B. Bell, P. Berrisford, S. Hirahara, A. Horányi, J. Muñoz-Sabater, J. Nicolas, et al. 2020. "The ERA5 Global Reanalysis." *Quarterly Journal of the Royal Meteorological Society* 146 (730): 1999–2049. https://doi.org/10.1002/qj.3803.

Inness, A., M. Ades, A. Agustí-Panaredaz, J. Barré, A. Benedictow, A. Blechschmidt, J. Dominguez, et al. 2019. "CAMS Global Reanalysis (EAC4)." Copernicus Atmosphere Monitoring Service. https://ads.atmosphere.copernicus.eu/cdsapp#!/dataset/cams-global-reanalysis-eac4?tab=overview.

IUCN (International Union for the Conservation of Nature). 2023. *The IUCN Urban Nature Indexes*. Gland, Switzerland: IUCN. https://doi.org/10.2305/RWDY8899.

Jing, C., M. Du, S. Li, and S. Liu. 2019. "Geospatial Dashboards for Monitoring Smart City Performance." *Sustainability* 11 (20): 5648. https://doi.org/10.3390/su11205648.

Joshi, P. 2017. "A Perspective on Education's Importance for Urban Development." *European Journal of Education* 52 (4): 421–26.

Kalluri, S., P. Gilruth, and R. Bergman. 2003. "The Potential of Remote Sensing Data for Decision Makers at the State, Local and Tribal Level: Experiences from NASA's Synergy Program." *Environmental Science & Policy* 6 (6): 487–500. https://doi.org/10.1016/j.envsci.2003.08.002.

Kampa, M., and E. Castanas. 2008. "Human Health Effects of Air Pollution." *Environmental Pollution* 151 (2): 362–67. https://doi.org/10.1016/j.envpol.2007.06.012.

Kavvada, A., G. Metternicht, F. Kerblat, N. Mudau, M. Haldorson, S. Laldaparsad, L. Friedl, et al. 2020. "Towards Delivering on the Sustainable Development Goals Using Earth Observations." *Remote Sensing of Environment* 247 (September): 111930. https://doi.org/10.1016/j.rse.2020.111930.

KBA Partnership (Key Biodiversity Areas Partnership). 2017. *The Relationship between Key Biodiversity Areas (KBAs) and Protected Areas*. Cambridge, UK: KBA Secretariat, Birdlife International. https://www.keybiodiversityareas.org/assets/8f1535aed3316ae2b720364019f8cb1c.

Kondo, M.C., S. Han, G.H. Donovan, and J.M. MacDonald. 2017. "The Association between Urban Trees and Crime: Evidence from the Spread of the Emerald Ash Borer in Cincinnati." *Landscape and Urban Planning* 157 (January): 193–99. https://doi.org/10.1016/j.landurbplan.2016.07.003.

Konijnendijk, C. 2021. "The 3-30-300 Rule for Urban Forestry and Greener Cities." *Biophilic Cities Journal* 4 (2): 2.

Kuffer, M., J. Wang, M. Nagenborg, K. Pfeffer, D. Kohli, R. Sliuzas, and C. Persello. 2018. "The Scope of Earth-Observation to Improve the Consistency of the SDG Slum Indicator." *ISPRS International Journal of Geo-Information* 7 (11): 428. https://doi.org/10.3390/ijgi7110428.

Kuffer, M., D.R. Thomson, G. Boo, R. Mahabir, T. Grippa, S. Vanhuysse, R. Engstrom, et al. 2020. "The Role of Earth Observation in an Integrated Deprived Area Mapping 'System' for Low-to-Middle Income Countries." *Remote Sensing* 12 (6): 982. https://doi.org/10.3390/rs12060982.

Lee, K.K., M.R. Miller, and A.S.V. Shah. 2018. "Air Pollution and Stroke." *Journal of Stroke* 20 (1): 2–11. https://doi.org/10.5853/jos.2017.02894.

Lind, L., E.M. Hasselquist, and H. Laudon. 2019. "Towards Ecologically Functional Riparian Zones: A Meta-analysis to Develop Guidelines for Protecting Ecosystem Functions and Biodiversity in Agricultural Landscapes." *Journal of Environmental Management* 249 (November): 109391. https://doi.org/10.1016/j.jenvman.2019.109391.

Litwiller, F., C. White, K. Gallant, S. Hutchinson, and B. Hamilton-Hinch. 2016. "Recreation for Mental Health Recovery." *Leisure/Loisir* 40 (3): 345–65. https://doi.org/10.1080/14927713.2016.1252940.

Ludwig, C., R. Hecht, S. Lautenbach, M. Schorcht, and A. Zipf. 2021. "Mapping Public Urban Green Spaces Based on OpenStreetMap and Sentinel-2 Imagery Using Belief Functions." *ISPRS International Journal of Geo-Information* 10 (4): 251. https://doi.org/10.3390/ijgi10040251.

Majeed, H., and J.S. Floras. 2022. "Warmer Summer Nocturnal Surface Air Temperatures and Cardiovascular Disease Death Risk: A Population-Based Study." *BMJ Open* 12 (3): e056806.

Malik, U., and W. James. 2007. "Reliability of Design Storms Used to Size Urban Stormwater System Elements." *Journal of Water Management Modeling* R227-16 (15): 309–26. https://doi.org/10.14796/JWMM.R227-16.

Martinuzzi, S., O.M. Ramos-González, T.A. Muñoz-Erickson, D.H. Locke, A.E. Lugo, and V.C. Radeloff. 2018. "Vegetation Cover in Relation to Socioeconomic Factors in a Tropical City Assessed from Submeter Resolution Imagery." *Ecological Applications* 28 (3): 681–93. https://doi.org/10.1002/eap.1673.

Martinuzzi, S., D.H. Locke, O. Ramos-González, M. Sanchez, J.M. Grove, T.A. Muñoz-Erickson, W.J. Arendt, et al. 2021. "Exploring the Relationships between Tree Canopy Cover and Socioeconomic Characteristics in Tropical Urban Systems: The Case of Santo Domingo, Dominican Republic." *Urban Forestry & Urban Greening* 62 (July): 127125. https://doi.org/10.1016/j.ufug.2021.127125.

Matthews, T., C. Raymond, J. Foster, J.W. Baldwin, C. Ivanovich, Q. Kong, P. Kinney, et al. 2025. "Mortality Impacts of the Most Extreme Heat Events." *Nature Reviews Earth & Environment* 6 (3): 1–18.

McDonald, R.I., M. Colbert, M. Hamann, R. Simkin, and B. Walsh. 2018. *Nature in the Urban Century: A Global Assessment of Where and How to Conserve Nature for Biodiversity and Human Wellbeing*. Arlington County, VA: The Nature Conservancy. https://www.nature.org/en-us/what-we-do/our-insights/perspectives/nature-in-the-urban-century/.

McFeeters, S.K. 1996. "The Rise of the Normalized Difference Water Index (NDWI) in the Delineation of Open Water Features." *International Journal of Remote Sensing* 17: 1425–32. https://doi.org/10.1080/01431169608948714.

Minion, S.C., E.E. Krans, M.M. Brooks, D.D. Mendez, and C.L. Haggerty. 2022. "Association of Driving Distance to Maternity Hospitals and Maternal and Perinatal Outcomes." *Obstetrics and Gynecology* 140 (5): 812–19.

Moreno, C., Z. Allam, D. Chabaud, C. Gall, and F. Pratlong. 2021. "Introducing the '15-Minute City': Sustainability, Resilience and Place Identity in Future Post-pandemic Cities." *Smart Cities* 4 (1): 93–111.

Myhre, G., D. Shindell, F.-M. Bréon, W. Collins, J. Fuglestvedt, J. Huang, D. Koch, et al. 2013. "Anthropogenic and Natural Radiative Forcing." In *Climate Change 2013: The Physical Science Basis.* Contribution of Working Group I to the Fifth Assessment Report of the Intergovernmental Panel on Climate Change, edited by T.F. Stocker, D. Qin, G.-K. Plattner, M. Tignor, S.K. Allen, J. Boschung, A. Nauels, et al., 659–740. Cambridge and New York: Cambridge University Press. https://www.ipcc.ch/site/assets/uploads/2018/02/WG1AR5_Chapter08_FINAL.pdf.

NASA (National Aeronautics and Space Administration). 2023. "NASA Earth Exchange Global Daily Downscaled Projections (NEX-GDDP-CMIP6)." August 27. https://www.nccs.nasa.gov/sites/default/files/NEX-GDDP-CMIP6-Tech_Note.pdf.

NASA JPL (NASA Jet Propulsion Laboratory). 2020. "NASADEM Merged DEM Global 1 Arc Second V001." Earth Engine Data Catalog. https://developers.google.com/earth-engine/datasets/catalog/NASA_NASADEM_HGT_001.

Nicoletti, L., M. Sirenko, and T. Verma. 2022. "Disadvantaged Communities Have Lower Access to Urban Infrastructure." *Environment and Planning B: Urban Analytics and City Science*, October. https://doi.org/10.1177/23998083221131044.

Niu, H., and E.A. Silva. 2020. "Crowdsourced Data Mining for Urban Activity: Review of Data Sources, Applications, and Methods." *Journal of Urban Planning and Development* 146 (2): 04020007. https://doi.org/10.1061/(ASCE)UP.1943-5444.0000566.

Nunes, A.R. 2024. "Heatwaves: The Silent Killers of Public Health." *Disaster Medicine and Public Health Preparedness* 18: e227.

Owen, D., A. Fitch, D. Fletcher, J. Knopp, G. Levin, K. Farley, E. Banzhaf, et al. 2024. "Opportunities and Constraints of Implementing the 3-30-300 Rule for Urban Greening." *Urban Forestry & Urban Greening* 98: 128393.

Pekel, J.-F., A. Cottam, N. Gorelick, and A.S. Belward. 2016. "High-Resolution Mapping of Global Surface Water and Its Long-Term Changes." *Nature* 540 (December): 418–22. https://doi.org/10.1038/nature20584.

Pereira, R.H.M., M. Saraiva, D. Herszenhut, C.K.V. Braga, and M.W. Conway. 2021. "R5r: Rapid Realistic Routing on Multimodal Transport Networks with R5 in R." *Findings*, March. https://doi.org/10.32866/001c.21262.

Pietilä, M., M. Neuvonen, K. Borodulin, K. Korpela, T. Sievänen, and L. Tyrväinen. 2015. "Relationships between Exposure to Urban Green Spaces, Physical Activity and Self-Rated Health." *Journal of Outdoor Recreation and Tourism* 10 (July): 44–54. https://doi.org/10.1016/j.jort.2015.06.006.

Pool, J.-R., D. Gibbs, S. Alexander, and N. Harris. 2022. "5 Reasons Cities Should Include Trees in Climate Action." *Insights* (blog), July 28. World Resources Institute. https://www.wri.org/insights/urban-trees-city-climate-action.

Potapov, P., M.C. Hansen, A. Pickens, A. Hernandez-Serna, A. Tyukavina, S. Turubanova, V. Zalles, et al. 2022. "The Global 2000–2020 Land Cover and Land Use Change Dataset Derived from the Landsat Archive: First Results." *Frontiers in Remote Sensing* 3 (April). https://doi.org/10.3389/frsen.2022.856903.

Prakash, M., S. Ramage, A. Kavvada, and S. Goodman. 2020. "Open Earth Observations for Sustainable Urban Development." *Remote Sensing* 12 (10): 1646. https://doi.org/10.3390/rs12101646.

Riahi, K., D.P. Van Vuuren, E. Kriegler, J. Edmonds, B.C. O'Neill, S. Fujimori, N. Bauer, et al. 2017. "The Shared Socioeconomic Pathways and Their Energy, Land Use, and Greenhouse Gas Emissions Implications: An Overview." *Global Environmental Change* 42 (January): 153–68. https://doi.org/10.1016/j.gloenvcha.2016.05.009.

Rodríguez-López, C., Z.M. Salas-Fariña, E. Villa-González, M. Borges-Cosic, M. Herrador-Colmenero, J. Medina-Casaubón, F.B. Ortega, et al. 2017. "The Threshold Distance Associated with Walking from Home to School." *Health, Education and Behavior* 44 (6): 857–66.

Rosenberg, E.A., P.W. Keys, D.B. Booth, D. Hartley, J. Burkey, A.C. Steinemann, and D.P. Lettenmaier. 2010. "Precipitation Extremes and the Impacts of Climate Change on Stormwater Infrastructure in Washington State." *Climatic Change* 102 (September): 319–49. https://doi.org/10.1007/s10584-010-9847-0.

Runfola, D., A. Anderson, H. Baier, M. Crittenden, E. Dowker, S. Fuhrig, S. Goodman, et al. 2020. "GeoBoundaries: A Global Database of Political Administrative Boundaries." *PLOS One* 15 (4): e0231866. https://doi.org/10.1371/journal.pone.0231866.

Salcedo-Sanz, S., P. Ghamisi, M. Piles, M. Werner, L. Cuadra, A. Moreno-Martínez, E. Izquierdo-Verdiguier, et al. 2020. "Machine Learning Information Fusion in Earth Observation: A Comprehensive Review of Methods, Applications and Data Sources." *Information Fusion* 63 (November): 256–72. https://doi.org/10.1016/j.inffus.2020.07.004.

Saraiva, M., R.H.M. Pereira, D. Herszenhut, C.K.V. Braga, M.W. Bhagat-Conway, and L. Liu. 2025. "Package r5r." Version 2.1.0. https://cran.r-project.org/web/packages/r5r/r5r.pdf.

Sathyakumar, V., R. Ramsankaran, and R. Bardhan. 2020. "Geospatial Approach for Assessing Spatiotemporal Dynamics of Urban Green Space Distribution among Neighbourhoods: A Demonstration in Mumbai." *Urban Forestry & Urban Greening* 48 (February): 126585. https://doi.org/10.1016/j.ufug.2020.126585.

Schimpl, M., C. Moore, C. Lederer, A. Neuhaus, J. Sambrook, J. Danesh, W. Ouwehand, et al. 2011. "Association between Walking Speed and Age in Healthy, Free-Living Individuals Using Mobile Accelerometry: A Cross-Sectional Study." *PLOS One* 6 (8): e23299.

Sekertekin, A. 2021. "A Survey on Global Thresholding Methods for Mapping Open Water Body Using Sentinel-2 Satellite Imagery and Normalized Difference Water Index." *Archives of Computational Methods in Engineering* 28 (3): 1335–47.

Shindell, D.T. 2015. "The Social Cost of Atmospheric Release." *Climatic Change* 130 (2): 313–26. https://doi.org/10.1007/s10584-015-1343-0.

Song, Y., and P. Wu. 2021. "Earth Observation for Sustainable Infrastructure: A Review." *Remote Sensing* 13 (8): 1528. https://doi.org/10.3390/rs13081528.

Song, D.X., Z. Wang, T. He, H. Wang, and S. Liang. 2022. "Estimation and Validation of 30 M Fractional Vegetation Cover over China through Integrated Use of Landsat 8 and Gaofen 2 Data." *Science of Remote Sensing* 6: 100058.

Stanley, T., and D.B. Kirschbaum. 2017. "A Heuristic Approach to Global Landslide Susceptibility Mapping." *Natural Hazards* 87 (May): 145–64. https://doi.org/10.1007/s11069-017-2757-y.

Sugiarto, W. 2022. "Impact of Wildlife Crossing Structures on Wildlife-Vehicle Collisions." *Transportation Research Record*, August. https://doi.org/10.1177/03611981221108158.

Terrestrial Ecosystems. n.d. "Species Accumulation Curves." https://terrestrialecosystems.com/species-accumulation-curves/. Accessed November 9, 2022.

Thomson, D.R., D.R. Leasure, T. Bird, N. Tzavidis, and A.J. Tatem. 2022. "How Accurate Are WorldPop-Global-Unconstrained Gridded Population Data at the Cell-Level? A Simulation Analysis in Urban Namibia." *PLOS One* 17 (7): e0271504. https://doi.org/10.1371/journal.pone.0271504.

Tolan, J., H.I. Yang, B. Nosarzewski, G. Couairon, H.V. Vo, J. Brandt, J. Spore, et al. 2024. "Very High Resolution Canopy Height Maps from RGB Imagery Using Self-Supervised Vision Transformer and Convolutional Decoder Trained on Aerial Lidar." *Remote Sensing of Environment* 300: 113888.

Tsendbazar, N., L. Li, M. Koopman, S. Carter, M. Herold, I. Georgieva, and M. Lesiv. 2021. *WorldCover Product Validation Report, Version 1.1*. Paris: European Space Agency. https://esa-worldcover.s3.eu-central-1.amazonaws.com/v100/2020/docs/WorldCover_PVR_V1.1.pdf.

UN (United Nations). n.d. "Goal 11." https://sdgs.un.org/goals/goal11. Accessed December 13, 2022.

Underwood, B.S., Z. Guido, P. Gudipudi, and Y. Feinberg. 2017. "Increased Costs to US Pavement Infrastructure from Future Temperature Rise." *Nature Climate Change* 7 (October): 704–7. https://doi.org/10.1038/nclimate3390.

UN DESA (UN Department of Economic and Social Affairs). 2022. *Methodology, United Nations Database on Household Size and Composition 2022*. UN DESA/POP/2022/DC/NO. 8. New York: United Nations.

UNEP-WCMC and IUCN (UN Environment Programme World Conservation Monitoring Centre and International Union for Conservation of Nature). n.d. (Database.) *Protected Planet: The World Database on Protected Areas (WDPA).* UNEP-WCMC and IUCN. https://www.protectedplanet.net/.

UN-Habitat (UN Human Settlements Programme). 2018. *SDG Indicator 11.2.1 Training Module: Public Transport System*. Nairobi: UN-Habitat.

UN-Habitat. 2020. *Metadata on SDGs Indicator 11.7.1.* Nairobi: UN-Habitat. https://unhabitat.org/sites/default/files/2020/11/metadata_on_sdg_indicator_11.7.1_02-2020_1.pdf.

UN-Habitat. 2022. *The Global Urban Monitoring Framework.* Nairobi: UN-Habitat. https://unhabitat.org/sites/default/files/2022/08/the_global_urban_monitoring_framework_metadata.pdf.

van der Kamp, J. 2017. *Social Cost-Benefit Analysis of Air Pollution Control Measures: Advancing Environmental-Economic Assessment Methods to Evaluate Industrial Point Emission Sources*. Karlsruhe, Germany: Karlsruher Institut für Technologie. https://doi.org/10.5445/KSP/1000072046.

van Donkelaar, A., M.S. Hammer, L. Bindle, M. Brauer, J.R. Brook, M.J. Garay, N.C. Hsu, et al. 2021. "Monthly Global Estimates of Fine Particulate Matter and Their Uncertainty." *Environmental Science & Technology* 55 (22): 15287–300. https://doi.org/10.1021/acs.est.1c05309.

van Oorschot, J., M. Slootweg, R.P. Remme, B. Sprecher, and E. van der Voet. 2024. "Optimizing Green and Gray Infrastructure Planning for Sustainable Urban Development." *npj Urban Sustainability* 4 (1): 41.

Volin, E., A. Ellis, S. Hirabayashi, S. Maco, D.J. Nowak, J. Parent, and R.T. Fahey. 2020. "Assessing Macro-scale Patterns in Urban Tree Canopy and Inequality." *Urban Forestry & Urban Greening* 55 (November): 126818. https://doi.org/10.1016/j.ufug.2020.126818.

Wang, C., Z.-H. Wang, and J. Yang. 2018. "Cooling Effect of Urban Trees on the Built Environment of Contiguous United States." *Earth's Future* 6 (8): 1066–81. https://doi.org/10.1029/2018EF000891.

Wang, Y., C. Huang, Y. Feng, M. Zhao, and J. Gu. 2020. "Using Earth Observation for Monitoring SDG 11.3.1-Ratio of Land Consumption Rate to Population Growth Rate in Mainland China." *Remote Sensing* 12 (3): 357. https://doi.org/10.3390/rs12030357.

Ward, P.J., H.C. Winsemius, S. Kuzma, M.F.P. Bierkens, A. Bouwman, H.D. Moel, A.D. Loaiza, et al. 2020. "Aqueduct Floods Methodology." Technical Note. Washington, DC: World Resources Institute. https://www.wri.org/research/aqueduct-floods-methodology.

Wellmann, T., A. Lausch, E. Andersson, S. Knapp, C. Cortinovis, J. Jache, S. Scheuer, et al. 2020. "Remote Sensing in Urban Planning: Contributions towards Ecologically Sound Policies?" *Landscape and Urban Planning* 204 (December): 103921. https://doi.org/10.1016/j.landurbplan.2020.103921.

Wesley, E.J., and N.A. Brunsell. 2019. "Greenspace Pattern and the Surface Urban Heat Island: A Biophysically-Based Approach to Investigating the Effects of Urban Landscape Configuration." *Remote Sensing* 11 (19): 2322.

WHO (World Health Organization). 2021. *WHO Global Air Quality Guidelines: Particulate Matter ($PM_{2.5}$ and PM_{10}), Ozone, Nitrogen Dioxide, Sulfur Dioxide and Carbon Monoxide*. Geneva: WHO. https://www.who.int/publications-detail-redirect/9789240034228.

Wilson, S.J., E. Juno, J.-R. Pool, S. Ray, M. Phillips, S. Francisco, and S. McCallum. 2022. *Better Forests, Better Cities*. Washington, DC: World Resources Institute. https://www.wri.org/research/better-forests-better-cities.

Wong, T., and P. Switzer. 2023. "Estimating Future Local Climate Hazard Probabilities." Technical Note. Washington, DC: World Resources Institute. https://doi.org/10.46830/writn.22.00074.

Wong, T., and E. Mackres. 2024. "City-Scale, City-Relevant Climate Hazard Indicators under 1.5°C, 2.0°C, and 3.0°C of Global Warming." Technical Note. Washington, DC: World Resources Institute. https://doi.org/10.46830/writn.23.00154.

WorldPop. n.d. "WorldPop Global Population Data." Earth Engine Data Catalog. https://developers.google.com/earth-engine/datasets/catalog/WorldPop_GP_100m_pop. Accessed November 8, 2022.

Xu, Z., G. FitzGerald, Y. Guo, B. Jalaludin, and S. Tong. 2016. "Impact of Heatwave on Mortality under Different Heatwave Definitions: A Systematic Review and Meta-analysis." *Environment International* 89–90 (April–May): 193–203. https://doi.org/10.1016/j.envint.2016.02.007.

Zanaga, D., R. Van De Kerchove, W. De Keersmaecker, N. Souverijns, C. Brockmann, R. Quast, J. Wevers, et al. 2021. "ESA WorldCover 10 M 2020 V100." *Zenodo*. https://doi.org/10.5281/zenodo.5571936.

Zeng, X., R.E. Dickinson, A. Walker, M. Shaikh, R.S. DeFries, and J. Qi. 2000. "Derivation and Evaluation of Global 1-km Fractional Vegetation Cover Data for Land Modeling." *Journal of Applied Meteorology 39* (6): 826–839. https://doi.org/10.1175/1520-0450(2000)039<0826:DAEOGK>2.0.CO;2.

Zerger, A., and D.I. Smith. 2003. "Impediments to Using GIS for Real-Time Disaster Decision Support." *Computers, Environment and Urban Systems* 27 (2): 123–41. https://doi.org/10.1016/S0198-9715(01)00021-7.

Zhang, M., S. Tan, C. Zhang, S. Han, S. Zou, and E. Chen. 2023. "Assessing the Impact of Fractional Vegetation Cover on Urban Thermal Environment: A Case Study of Hangzhou, China." *Sustainable Cities and Society* 96: 104663.

Acknowledgments

This research was made possible by the UrbanShift and Cities4Forests initiatives. We are thankful for the financial support of those initiatives from the Global Environment Facility and the United Kingdom Department for Environment, Food & Rural Affairs, respectively, which supported this research.

The authors would like to thank the reviewers and advisers who provided input on this research (unless otherwise noted, organizational affiliations are WRI): Becky Atkins, Ignacio Bernabe, Alejandra Bosch, Beatriz Cárdenas, Ingrid Coetzee (ICLEI), Gennadii Donchyts (Google), Jessica Ertel, Catyana Falsetti, Gloria Ferreyra, David Gibbs, Argyro Kavvada (NASA), Robin King, Samantha Kuzma, Jiaying Lin, Marc Manyifika, John-Rob Pool, Jaap Schellekens (Planet), Bongiwe Simka (ICLEI), Gregory Taff, Wubanchi Tesso, and Mthobisi Wanda (ICLEI). Additionally, we would like to thank representatives of participant cities and liaisons who provided input on this research and presentations of the findings through surveys, focus groups, and interviews: Suryani Amin (ICLEI), Jessy Appavoo (C40 Cities), Ignacio Bernabe, Lara Caccia, Constant Cap (Code for Africa), Héctor Miguel Donado, Roger Mambeta Ndona, Bhaskar Padigala (ICLEI), Wubanchi Tesso, and Ji Xu (ICLEI).

Thanks also to the advisory group for the geospatial and data governance work of UrbanShift: Christoph Aubrecht (ESA), Zoltan Bartalis (ESA), Merlin Chatwin (Open North), Thomas Esch (German Aerospace Center), Dennis Mwaniki (UN-Habitat), Laura Parry (CDP), Steven Ramage (Group on Earth Observations), Stefaan Verhulst (New York University GovLab), and Dylan Weakley (City of Johannesburg).

Thanks also to the WRI program, technical, and operational staff who made this work and publication possible: Sadof Alexander, Timothy Anderegg, James Anderson, Logan Byers, Marc Daniels, Todd Gartner, Christopher Gillespie, Bruno Hernandez Incau, Manal Khan, Pablo Lazo, Beth Olberding, Mariana Orloff, John-Rob Pool, Emilia Suarez, and Deborah Valencia.

About the Authors

Eric Mackres is senior manager for urban analytics and data innovation at WRI Ross Center for Sustainable Cities.

Ted Wong is a research and project associate on the Urban Analytics and Data Innovation team at WRI Ross Center for Sustainable Cities.

Saif Shabou is an urban data and analytics associate on the Urban Analytics and Data Innovation team at WRI Ross Center for Sustainable Cities.

Elizabeth Jane Wesley is a data scientist, urban surfaces and extreme heat, at WRI Ross Center for Sustainable Cities.

Thet Hein Tun is a senior transportation research associate at WRI Ross Center for Sustainable Cities.

About WRI

World Resources Institute works to improve people's lives, protect and restore nature, and stabilize the climate. As an independent research organization, we leverage our data, expertise, and global reach to influence policy and catalyze change across systems like food, land and water; energy; and cities. Our 2,000+ staff work on the ground in more than a dozen focus countries and with partners in over 50 nations.